ASSESSMENT OF TISSUE ELASTICITY ON DIFFERENT SHEAR WAVE ULTRASOUND ELASTOGRAPHY (SWE) MODALITIES

NUR AMIRAH AMIR

MASTER OF MEDICAL PHYSICS
PROJECT RESEARCH REPORT
FACULTY OF MEDICINE
UNIVERSITY OF MALAYA
KUALA LUMPUR

2018

ASSESSMENT OF TISSUE ELASTICITY ON DIFFERENT SHEAR WAVE ULTRASOUND ELASTOGRAPHY (SWE) MODALITIES

NUR AMIRAH AMIR

PROJECT REPORT SUBMITTED IN PARTIAL FULFILMENT OF THE REQUIREMENTS FOR THE DEGREE OF MASTER OF MEDICAL PHYSICS

FACULTY OF MEDICINE
UNIVERSITY OF MALAYA
KUALA LUMPUR

2018

UNIVERSITY OF MALAYA

ORIGINAL LITERARY WORK DECLARATION

Name of Candidate: Nur Amirah binti Amir

Matric No: MGQ 170008

Name of Degree: Master of Medical Physics

Title of Project Paper/Research Report/Dissertation/Thesis:

Assessment of Tissue Elasticity on Different Shear Wave Ultrasound Elastography (SWE) Modalities

Field of Study: Medical Physics

I do solemnly and sincerely declare that:

(1) I am the sole author/writer of this Work;
(2) This Work is original;
(3) Any use of any work in which copyright exists was done by way of fair dealing and for permitted purposes and any excerpt or extract from, or reference to or reproduction of any copyright work has been disclosed expressly and sufficiently and the title of the Work and its authorship have been acknowledged in this Work;
(4) I do not have any actual knowledge nor do I ought reasonably to know that the making of this work constitutes an infringement of any copyright work;
(5) I hereby assign all and every rights in the copyright to this Work to the University of Malaya ("UM"), who henceforth shall be owner of the copyright in this Work and that any reproduction or use in any form or by any means whatsoever is prohibited without the written consent of UM having been first had and obtained;
(6) I am fully aware that if in the course of making this Work I have infringed any copyright whether intentionally or otherwise, I may be subject to legal action or any other action as may be determined by UM.

Candidate's Signature Date:

Subscribed and solemnly declared before,

Witness's Signature Date:

Name:

Designation:

ABSTRACT

Shear wave elastography (SWE) is one of the new elastography imaging techniques which uses ultrafast ultrasound to measure and visualise tissue elasticity. This study was conducted to measure and verify the SWE measurement in a gelatine-based elasticity phantom. Five spherical inclusions of different sizes (2.9 cm and 4.5 cm) and different masses were constructed by mixing (5 to 25 g with 5 g increments) gelatine with 0.5 g of $CaCO_3$ (as scatterer) in 150 ml of distilled water. Different amounts of gelatine represent different stiffness of lesions. 80 g of gelatine was used to construct background phantom which was mixed with 800 ml of water. The lesions were placed inside the background phantom at two different depths of different containers. The lesions' elasticity was measured using three elastography modalities; Ultrasound Philips (iU22, Philips, USA), Ultrasound Supersonic (Aixplorer V6, Supersonic Imagine, France) and Fibroscan® (Fibroscan 502 Touch, Echosense, France). There were then compared with the gold standard measurement from a tensile testing machine Instron (Model 5969 Dual Column, Instron Co, USA). Elasticity measured using the Supersonic method showed stronger correlation than elasticity measured using Ultrasound Philips. No valid measurement was obtained from Fibroscan®, however an examination was performed on a volunteer to observe the procedure in Fibroscan and the elasticity value. The modulus of elasticity measured using Instron microtester were 1.6, 5.39, 11.84, 15.17 and 63.57 kPa respectively. The comparison between SWE ultrasound showed no significant difference ($p>0.05$) for 4.5 cm lesions at both 2 cm and 5 cm depth. There was a significant difference ($p<0.05$) of mean of elasticity between both ultrasound and Instron microtester. Results also showed that the tissue elasticity was overestimated for both ultrasound when compared with the gold standard.

Keywords: shear wave elastography (SWE), elasticity, lesion, ultrasound, gold standard

ABSTRAK

Shear wave elastography (SWE) adalah salah satu teknik *elastography* yang menggunakan *ultrafast ultrasound* untuk mengukur dan mengambarkan kekenyalan tisu dalam kawasan yang ditetapkan. Kajian ini telah dijalankan untuk mengkaji dan mengesahkan pengukuran *SWE* kekenyalan fantom yang diperbuat daripada gelatin (gel). Lima acuan sphera yang terdiri daripada size (2.9 cm dan 4.5 cm) dan berat yang berbeza telah dihasilkan daripada campuran (5 hingga 25 g dengan kenaikan 5 g) gelatin (gel) dengan 0.5 g $CaCO_3$ dengan 150 ml air suling. Berat gelatin yang berbeza mewakili kekenyalan ketumbuhan yang berbeza. 80 g gelatin telah di gunakan untuk menghasilkan fantom (latar belakang) dengan mencapurkan 800 ml air. Ketumbuhan- ketumbuhan tersebut telah diletakkan ke dalam fantom (latar belakng) pada dua kedalaman yang berbeza dalam dua bekas. Kekenyalan ketumbuhan- ketumbuhan tersebut telah diukur mengunakan tiga mesin *elastography*; Ultrasound Philips (iU22, Philips, USA), Ultrasound Supersonic (Aixplorer V6, Supersonic Imagine, France) dan Fibroscan® (Fibroscan 502 Touch, Echosense, France). Kemudian kekenyalan akan dibandingkan dengan pengukuran *gold standard* daripada mesin *tensile testing* Instron (Model 5969 Dual Column, Instron Co, USA). Kekenyalan yang diukur dengan Supersonic menunjukkan terdapat hubungan yang kukuh antara kedua-dua pengukuran berbanding dengan kekenyalan yang diukur menggunakan Ultrasound Philips. Tiada pengukuran tetap yang diterima daripada Fibroscan®, namun satu permeriksaan telah dijalankan terhadap seorang sukarela untuk melihat cara-cara pengunaan Fibroscan dan kekenyalan *Modulus* kekenyalan yang diukur mengunakan Instron *microtester* masing- masing adalah 1.6, 5.39, 11.84, 15.17 and 63.57 kPa respectively. Perbandingan antara *SWE ultrasound* tiada siknifikan berbeza ($p>0.05$) untuk ketumbuhan 4.5 cm pada kedalaman 2 cm and 5 cm. Terdapat signifikasi berbeza ($p<0.05$) pada purata kekenyalan antara

ultrasound dan Instron *microteste*r. Hasil menunjukkan kekenyalan tisu telah terlebih anggaran untuk kedua-dua *ultrasound*s apabila dibandingkan dengan *gold standard*.

ACKNOWLEDGEMENTS

My enthusiasm to conduct this research project came from the supports and helps from people around me. Without their help I would never been able to complete this research project. I humbly thanks God, whom with His willing had giving me the opportunity to complete this report.

Firstly, would like to express my deepest gratitude to my supervisor, Dr. Yeong Chai Hong, who had guided me during this project. Without her assistance and dedicated involvement in every step through this process, this research project would never been accomplished. My sincere thanks go to my co-supervisor Professor Ng Kwan Hoong for their continuous guidance and advice in helping me towards improvement of this project.

Next, I wish to express my sincere thanks to radiologist, sonographer and lab assistance that involved for their helps and supports during this research period. Upon completion of this research project, I would like to express my appreciation to my family for their cooperation, encouragement, suggestion and support. Also thanks to my classmates any anyone who contribute to my research project directly or indirectly. I would like to acknowledge their comments and suggestions which is crucial for the successful completion of this study.

TABLE OF CONTENTS

LIST OF FIGURES

LIST OF TABLES

LIST OF SYMBOLS AND ABBREVIATIONS

σ	:	Stress
ε	:	Strain
ρ	:	density
^{o}C	:	Degree celcius
ARFI	:	Acoustic Radiation Force Impulse
c_s	:	Shear wave speed
CAP	:	Controlled Attenuation Parameter
$CaCO_3$	:	Calcium Carbonate
cm	:	Centimetre
E	:	Modulus of Elasticity / Young's Modulus
F	:	Force
g	:	Gram
G	:	Shear modulus
Hz	:	Hertz
k	:	Spring constant
kg	:	Kilo gram
kN	:	Kilo Newton
kPa	:	Kilopascal
mm	:	Millimetre
ms	:	Millisecond
r	:	Pearson's correlation
R^2	:	Coefficient of determination
ROI	:	Region of interest
rpm	:	Revolutions per minutes

SWE	:	Shear wave Elastography
SWI	:	Shear wave Imaging
TE	:	Transient Elastography
US	:	Ultrasound
UMMC	:	University Malaya Medical Centre
x	:	Displacement

LIST OF APPENDICES

CHAPTER 1: INTRODUCTION

1.1 Introduction

Ultrasonography is a diagnostic technique which is reverence and commonly use in medical imaging due to its easy to handle and operate, real-time capability, portable and low cost (Gennisson, *et al.*, 2013). Ultrasonography uses ultrasound that produces high frequency waves which allow the formation of a morphological image of visceral organs. Ultrasound can be used as an alternative method to replace current clinical examination such as biopsy and palpation technique which can be destructive and caused pain to the patient. However ultrasound has a limitation as the wave propagation is homogeneous towards all tissue and cannot provide any information on tissue stiffness (Gennisson, *et al.*, 2013). Therefore, ultrasound elastography was developed to study tissue elasticity and replace the physical examination performed by clinicians.

Ultrasound elastography is used in reflecting the stiffness of target tumor and tissue characterisation. According to Lee *et al.* (2012) and Chang *et al.* (2011), this imaging technique improves the accuracy of diagnostic performance in conventional ultrasound especially in breast tissue characterisation. However, the elasticity image produced by elastography is highly dependent on the organ's compressibility limits under stress and on the extent of tissue the force is applied to (Chang *et al.*, 2011). Thus, it will show an estimated measurement of local strain which is not the quantitative information needed. A quantitative elastography method which is shear wave elastography (SWE) has been developed to improve the specification of elastography (Gennisson, *et al.*, 2013; Lee *et al.*, 2012; Chang *et al.*, 2011).

In the shear wave's method, standard ultrasound transducers track the shear wave that travels through the tissues and the speed can be measured. Shear wave propagation enables quantitative determination of tissue elasticity from the velocity of the wave as it

travels through the tissue. The speed travels increase with increasing tissue elasticity and this allows the estimation of Young's modulus (elasticity) (Lescheid *et al.*, 2015). The measurement of tissue elasticity is shown in kilopascals (kPa) or metres per second (m/s).

1.2 Significance of Study

Ultrasonic imaging techniques are the subject of intense research activity and the capabilities of new approaches to provide more information of considerable actual and potential clinical value are highly attractive. This study can provide justification knowledge about soft tissue elasticity measured using shear wave elastography (SWE) ultrasound system. The accuracy of tissue elasticity measured were compared to gold standard which can be improved from previous study and thus can be used in diagnostic application. Shear wave ultrasound elastography (SWE) was also compared with other machines; Fibroscan® and Instron tensile machine, to provide information about the accuracy, quality and tissue elasticity parameters such as size, distance and stiffness.

1.3 Objectives

The main objectives of this study were;

1. To design and develop a tissue-mimicking phantom stimulating varying sizes, stiffness and depth from the surface on the elasticity measurement using shear wave elastography (SWE) ultrasound.
2. To determine the accuracy of tissue elasticity measured by comparing the values with different systems; Instron (Gold Standard) and Fibroscan®.

CHAPTER 2: LITERATURE REVIEW

2.1 Elastography

Elastography is a new dynamic medical imaging application technique that use ultrasound to map and visualise the elastic properties and stiffness of soft tissue. According to Wells and Liang (2011), elastography gives the main information whether the tissue is hard or soft which will give diagnostic information about the presence or status of disease. Romagnulo (2011) and Cozens (2011) stated that elastography use transducer compression technique which connect with ultrasound and caused the deformation of small structure detected within the B-mode image. The degree of distortion measured provides the estimation of tissue stiffness. This medical imaging use the physics principle of Young's E modulus, which is the physical parameter related to tissue stiffness. Therefore, elastography was developed to measure tissue stiffness and he mapping of the tissue stiffness can be estimated either from the strain in the tissue under stress (quasi-static methods) or by the mechanical wave which propagation dependent by tissue stiffness (shear wave elastography) (Gennisson *et al.*, 2013).

Quasi- static technique is used when constant stress or force is slowly applied so that the structure deforms also very slowly (very low strain rate) and therefore the inertia force is very small and can be ignored. According to Gennisson *et al.* (2013), two-dimesional (2D) correlation of ultrasound images is estimated based on strain and displacement generated. Young's modulus which links with stress and stress in pure elastic medium, obeys Hook's Law:

$$\sigma = E\varepsilon \qquad \text{Equation (1)}$$

Where σ is the stress/force applied on the material, ε is the strain in material and E is the Young's Modulus of Elasticity. This quasi-static technique can easily implemented

but the stress distribution could prevents quantitative estimation of the Young's Modulus (kPa).

Based on physics theory, dynamic or mechanical waves, cause a structure to vibrate and the inertia force is big enough and that it must be considered (Sarvazyan *et al.*, (1995). Paparo *et al.* (2014) and Garra *et al.* (1997) state that, there are two type of time-varying force which are short transient mechanical force or oscillatory force with fixed frequency can be applied to the tissue. Figure 2.1 shows force which propagate through tissue as compresssional waves. According to Gennission *et al.* (2013) and Sigrist (2017), compressional waves or shear waves can propagate through the human body very quickly (~1500 m/s) and this wave can be used to visualise the body at a high frequencies. However at this high frequencies wave travels more slowly due to absorption therefore shear wave is generated at only low frequencies which range between (10 Hz to 2000 Hz).

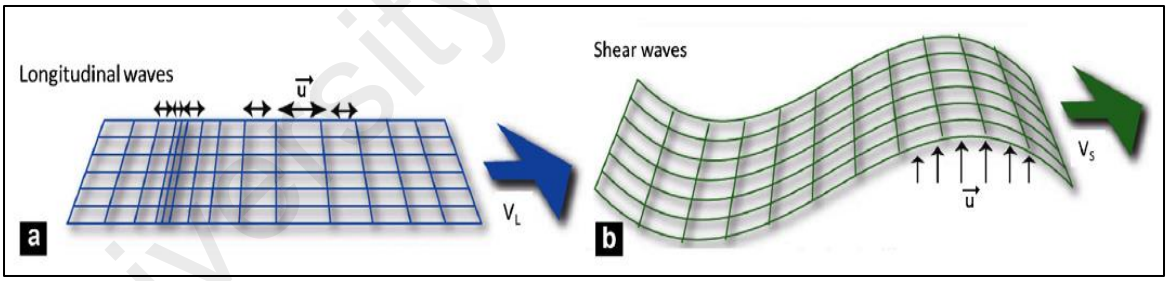

Figure 2.1 (a) Longitudinal wave use in ultrasound and sound wave **(b)** Shear wave travel at perpendicular direction of propagation (Adapted from Gennisson *et al.*, 2013)

2.2 Ultrasound (US) Elastography Technique

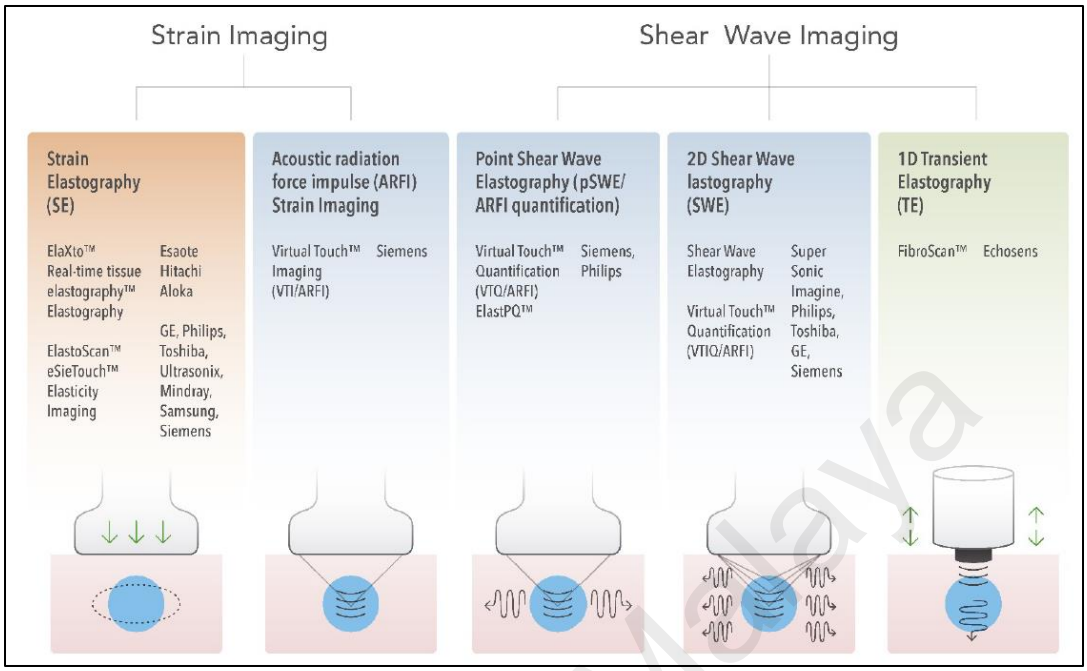

Figure 2.2 Ultrasound classification based on elastography technique (Adapted from Sigrist *et al.*, 2017)

Based on quasi-static and dynamic elastography, Figure 2.2 shows current US elastography technique been classified by the measured physical quantities. In strain imaging, a normal stress/ force is applied to the tissue and the strain is obtained, based on equation 1, measurement of Young's modulus can be calculated (Sigrist *et al.*, 2017. Shear wave imaging (SWI) is a mechanical wave which can be generated from acoustic radiation force impulse (ARFI) via focused ultrasound beam (Gennisson, *et al.*, 2013; Leschied *et al.*, 2015 & Lee *et al.*, 2012). Stress which is applied to the tissue using transducer/probe in 1D transient elastography (TE) or ARFI and 2D shear wave elastography. Based on figure 2.2, 2D shear wave is generated and measured perpendicular to the acoustic radiation force meanwhile 1D transient elastography excitation is measured parallel to the acoustic radiation force. The Young's modulus can be measured using equation:

$$E = 3G = 3\rho c_s^2 \qquad \text{Equation (2)}$$

Where G is the shear modulus, density, ρ has unit of kg/m^3 and c_s^2 is shear wave speed in m/s. In this study, a shear waves imaging technique was focused and used to measure the elasticity. Acoustic radiation force is an acoustic ''pushing pulse'' which is used to displace tissue (which displacement of ~10-20 μm) in the normal direction.

Shear wave imaging (SWI) measured displacement of tissue which is parallel to the stress applied. SWI uses dynamic stress to generate shear waves in both parallel (transient) and perpendicular dimension. Estimation of tissue elasticity can be measured from shear wave speed. According to Nightingale *et al.* (2003), there are currently three technical approaches in SWI which are 1D transient elastography, point shear wave and 2D shear wave.

2.2.1 1D Transient Elastography (TE)

One of the classification of shear wave elastography technique is transient elastography (TE). Transient elastography use the basic principle of wave propagation velocity through tissue. According to Yeh *et al.* (2002), a vibration of mild amplitude and low frequency (50 Hz) is produced when an ultrasound transducer mounted on the axis of the vibrator, consequently inducing an elastic shear wave that propagates through the tissue. Pulse-echo ultrasound follows the propagation of the shear wave and measures its velocity, which is related to tissue stiffness. Sporea *et al.* (2011) stated that, the velocity of waves travel through tissue correlates with tissue stiffness thus provides data about the condition and stiffness of the liver; wave travel faster through denser, fibrotic tissue. Figure 2.3 showed the wave propagation through tissue parallel to the acoustic radiation force.

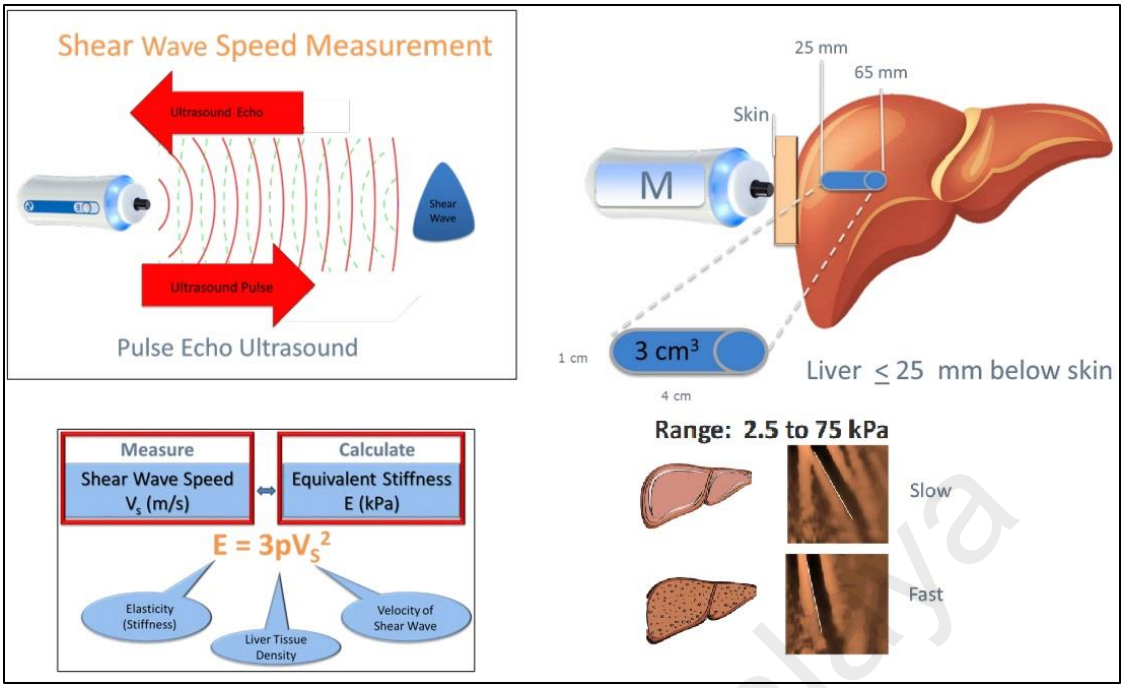

Figure 2.3 Waves travel parallel to the Acoustic Radiation Force

(Adapted from Samuel, 2016)

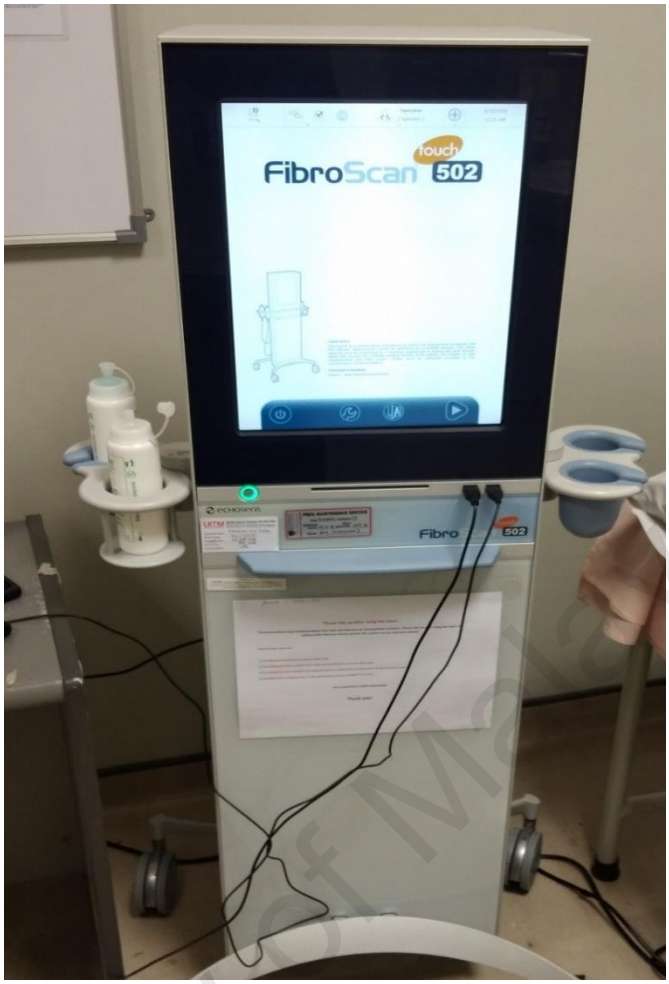

Figure 2.4 Fibroscan® manufacturer by Echosense at UMMC

Fibroscan is one of the modality that use transient elastography (TE) technique (Figure 2.4). Fibroscan has been introduced and reported in 2003 as one the ultrasound-based modality for quantitative assessment of liver fibrosis. Jung and Kim (2012) stated that, the amount of fibrosis in liver can be determine by the homogenous tissue which is proportional to its elasticity. The results are immediately obtained after performance of TE and expressed in kilopascals (kPa), corresponding to the median value of 10 validated measurements (range 2.5-75 kPa) (Wilder & Patel, 2014). It is reported that the velocity of elastic waves is faster in fibrotic liver than normal livers in previous study.

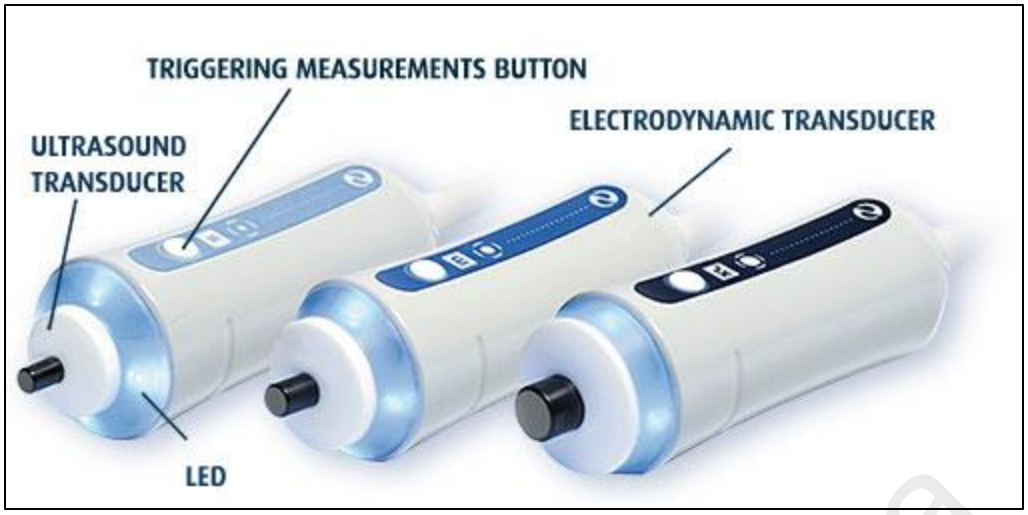

Figure 2.5 Fibroscan's probe with variety sizes (S, E and XL) (Adapted from Samuel, 2016)

Figure 2.5 shows variety sizes of fibroscan probe; small (S) for pediatrics and $^{+}$E and XL^{+} for adults. Friedrich-Rust *et al.* (2009) mentioned that, in adults, the wave propagate from the probe can penetrate the skin and travel from 25 mm to 75 mm to the liver. This probe managed to scan 3cm^3 of liver tissue to be measured and with this large area the measurement is almost accurate.

2.2.2 Two–dimensional (2D) Shear Wave Elastography

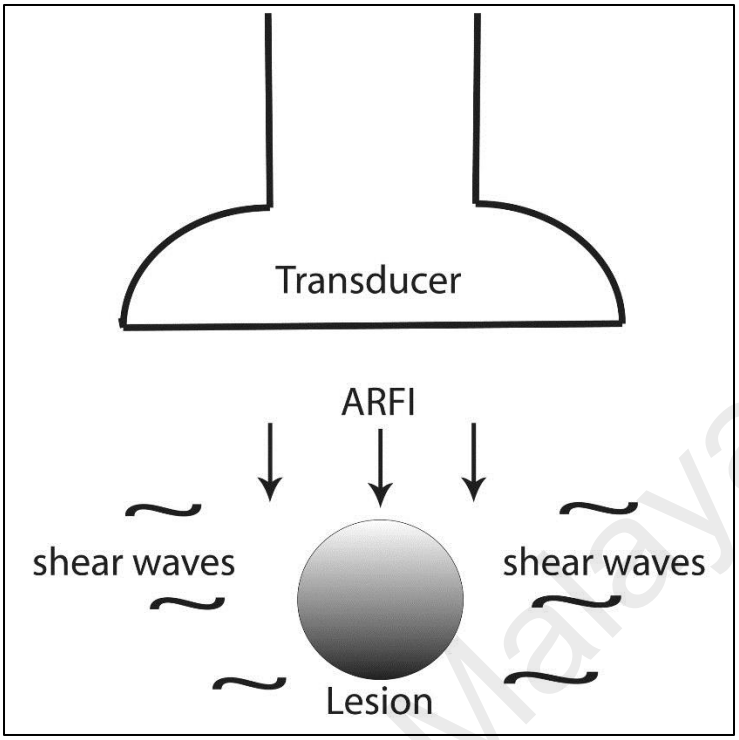

Figure 2.6 Two-dimensional shear wave propagation

2D SWE which uses acoustic radiation force is one of the newest SWI techniques. This technique allows real time monitoring and creation of elastic maps of tissue. Besides that this technique also provides real-time visualisation of a colour quantitative elastogram superimposed on B-mode image and enabling the operator to be guided by both anatomical and tissue stiffness information. Figure 2.6 showed basic idea on how the 2D shear wave is generated. There are two ultrasound modalities provided with shear wave mode; US Philips and US Supersonic. SWE Philips is designed to the measure the elasticity of tissue in addition the velocity of the shear wave can also automatically be obtained during examination.

Besides SWE Philips, SWE Supersonic also innovated and developed with SWE mode. In advance this system provide a colour map for the tissue. The stiffness of the tissue can be determine by the colour showed on the monitor (red, blue/green and blue). Supersonic can examine large area of ROI compared to SWE Philips which ROI is only

about 1.5 cm x 1.5 cm. According to Fink (2010) and Sebag (2010), at a very high frame rate, which is up to 20,000 frames per second, successive real time frequency dots are captured by using an ultrafast echo graphical sequence.

(a) (b)

Figure 2.7 (a) SWE Philips iU22 **(b) SWE** Supersonic Imagine (Adapted from Dhyani *et al.*,2015)

2.3 Elasticity

Elasticity can be defined as the property of a body by which it experiences a change in size or shape when a force acts on its body. The basic principle of elasticity is based on Hooke's Law which basically refer to the extension and compression of spring when certain force is applied on in.

$$F = kx \qquad \text{Equation 3}$$

Where F is the force applied on the spring, k is the spring constant and x is the displacement of the spring from its original position.

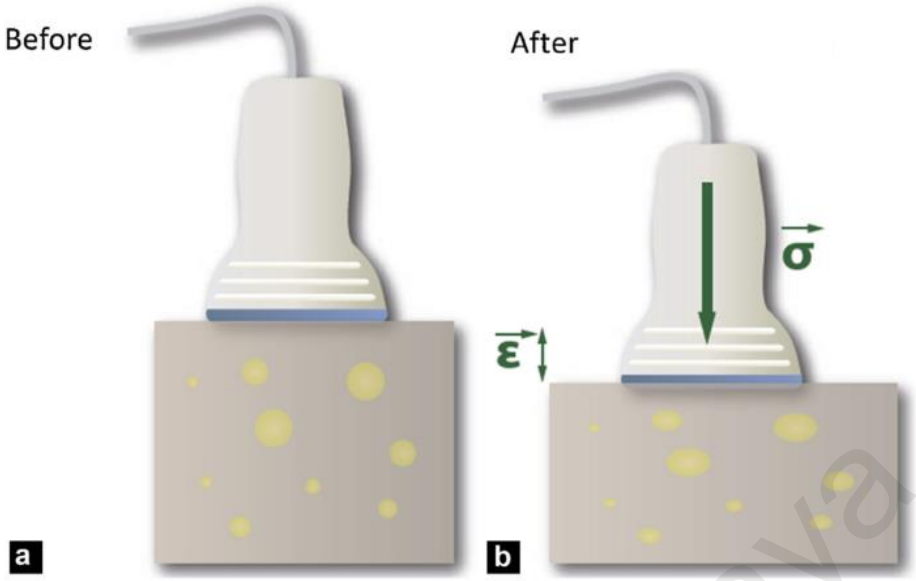

Figure 2.8 Deformation of material **(a)** before and **(b)** after a force acting on it (Adapted from Gennisson *et al.*, 2013)

According to Gennisson *et al.* (2013), a force is applied to the area of the medium and the strain induced is obtained from the difference between the before and after the force is applied. Figure 2.8 shows the strain obtained after the force is applied. The force applied toward the material is known as stress, σ and the deformation of medium is known as strain. If the deformation is small, therefore elasticity or Young's modulus of a material can be obtained from Hooke's law based on the equation (1). However Hooke's Law describe only the initial linear portion of the stress-strain graph for a bar subjected to uniaxial extension meanwhile Young's modulus is obtained from the slope of the straight line portion of stress-strain curve. Based on equation (1), Young's modulus is measured the elastic modulus when the object deformed after the compressional stress is applied parallel to it and by rearrange equation (1), Modulus of Elasticity or Young's Modulus is the ratio of applied stress to the strain of a material:

$$E = \frac{\sigma}{\varepsilon}$$ Equation (4)

D'angelo (1975) and Maksuti *et al.* (2016) state that, the bigger the Young's Modulus the stiffer the material is and when the tissue is hardly compressed the *E* is higher.

CHAPTER 3: METHODOLOGY

3.1 Introduction

The flow of the determination of the tissue elasticity on different parameters; stiffness, size and depth from the surface using shear wave elastography (SWE) ultrasound are described in this chapter. The methodology is divided into four major steps which are (1) preparation and development of tissue phantom, (2) construction of phantom background, (3) measurement of tissue elasticity and (4) comparison of elasticity values across different machines. The flowchart which shows the overview of this project is shown in figure 3.1.

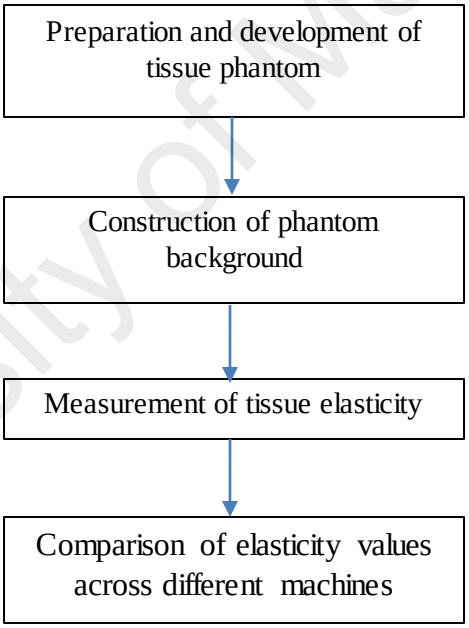

Figure 3.1 The flow chart of the study

3.2 Materials

The materials used in the research were divided into three categories which are chemical, equipment and instrumentation; and apparatus and glassware.

3.2.1 Chemicals

The list of chemicals used are:

Calcium carbonate, $CaCO_3$,

Distilled water,

Food colouring- Red and Green (CI 14720, Tesco, Malaysia),

Gelatin powder (JC Rainbow Enterprise, Selangor),

Sky gel (USSKYGEL260G, ISD Meditech SDN. BHD., Selangor)

3.2.2 Apparatus and Glassware

The list of apparatus used are:

Beaker,

Food Container (3.5 L),

Magnetic stirrer,

Masking tape,

Mould

3.2.3 Equipment and Analytical Instruments

The list of equipment and analytical instruments used are:

Analytical balance (FX-300i, A&D Co., LTD, Japan),

Chiller,

Fibroscan (Fibroscan 502 Touch, Echosens, France),

Hot plate (MR-Hei-Standard, Heidoplh Instruments, Germany),

Instron Tensile Machine (Model 5969 Dual Column, Instron Co, USA),

SWE Ultrasound Philips (iU22, Philips, USA),

SWE Ultrasound Supersonic (Aixplorer V6, Supersonic Imagine, France)

3.3 Methods

3.3.1 Preparation and Development of Tissue Phantom

Phantoms of different elasticity were constructed by mixing both gelatine powder and calcium carbonate, $CaCO_3$. The amount of $CaCO_3$ were fixed at 0.5 g meanwhile the mass of gelatine powder were increased according to the elasticity needed. $CaCO_3$ was used as a stabilizer and preservative for the tissue phantoms. The steps for preparation and development of tissue phantom are illustrated as follows:

1. 150 ml of distilled water was measured and transferred into 60 ml beaker.
2. The water was heated up to 100°C on a hot plate.
3. 5 g of gelatine powder and 0.5 g of $CaCO_3$ were measured and added into the heated water. The mixture were mixed and stirred by using magnetic stirrer at 400 rpm on the hot plate. The aqueous gelation solution was obtained until all the gelatine was completely dissolved. The mixing process of $CaCO_3$ and gelatine was showed in figure 3.2.
4. Formation of bubbles during the mixing and stirring were removed by using spatula.
5. The mixing and stirring process was stopped once the aqueous gelatine solution turned into molten gelatine.
6. A few drops of green food colouring was added into the aqueous gelatine solution to differentiate between inclusion and background.
7. The beaker of molten gelatine was removed from hot plate and transferred into a cold water bath. The beaker was partially immersed to cool down the temperature of the molten gelatine.
8. After the molten gelatine was cooled, the molten gelatine was poured into 100 mL beaker. 2 hemispherical scoop which will shaped into spherical moulds with a diameter of 2.9 cm was dipped into the molten gelatine and clamped together to

form spherical inclusion. Formation of bubbles should be avoided when dipping the moulds.

9. The beaker was kept in the chiller (4°C) for cooling and further congealed.
10. After the gelatine was congealed, the spherical moulds were removed from the beaker and the spherical gelatine was carefully removed.
11. Steps 1 to 10 were repeated by changing the size of the mould (diameter 2.9 cm) to mould with diameter of 4.5 cm. Figure 3.3 showed step by step procedure of preparation and development of lesion
12. Steps 1 to 11 were repeated to increase the elasticity of the inclusion by using different amount of gelatine; 10, 15, 20 and 25 g. For each mass of gelatine, the food colouring added was alternately changed to differentiate from one another.

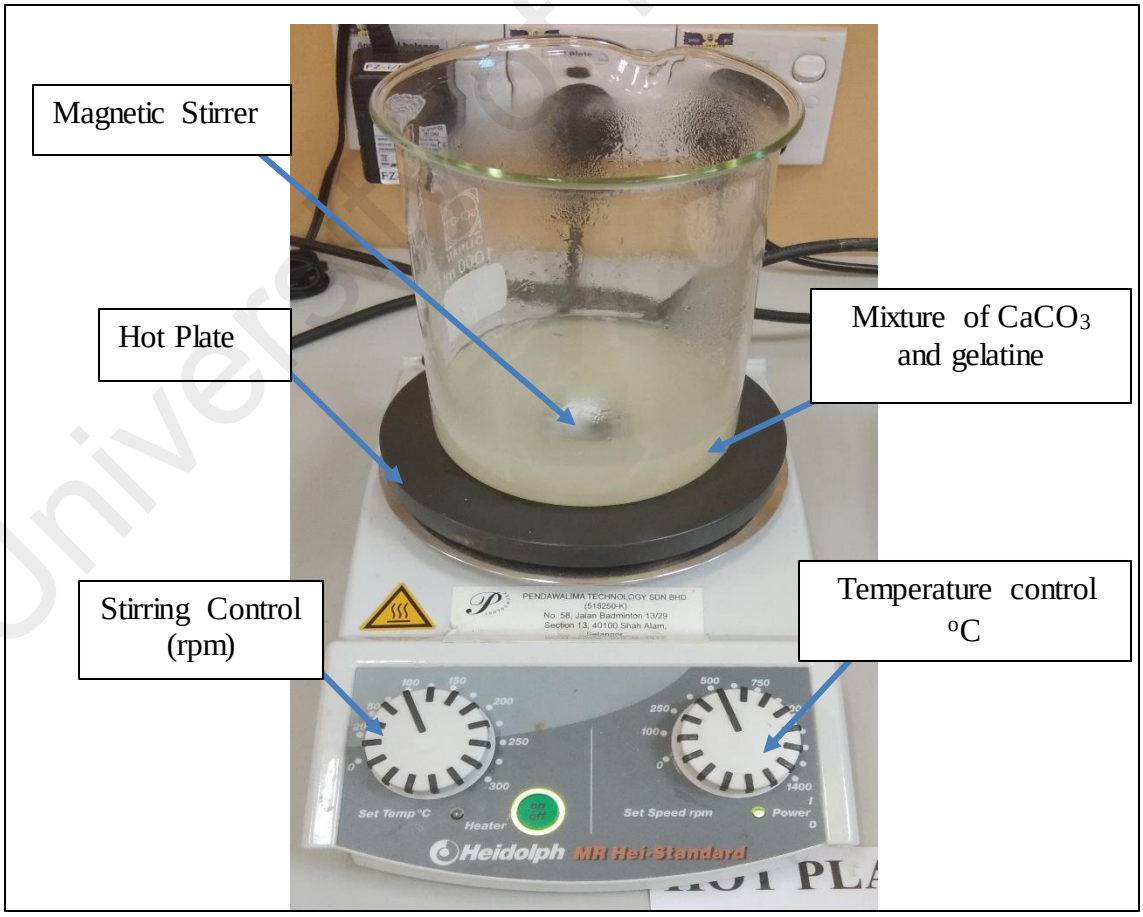

Figure 3.2 Mixing process of $CaCO_3$ and gelatine to construct spherical inclusion

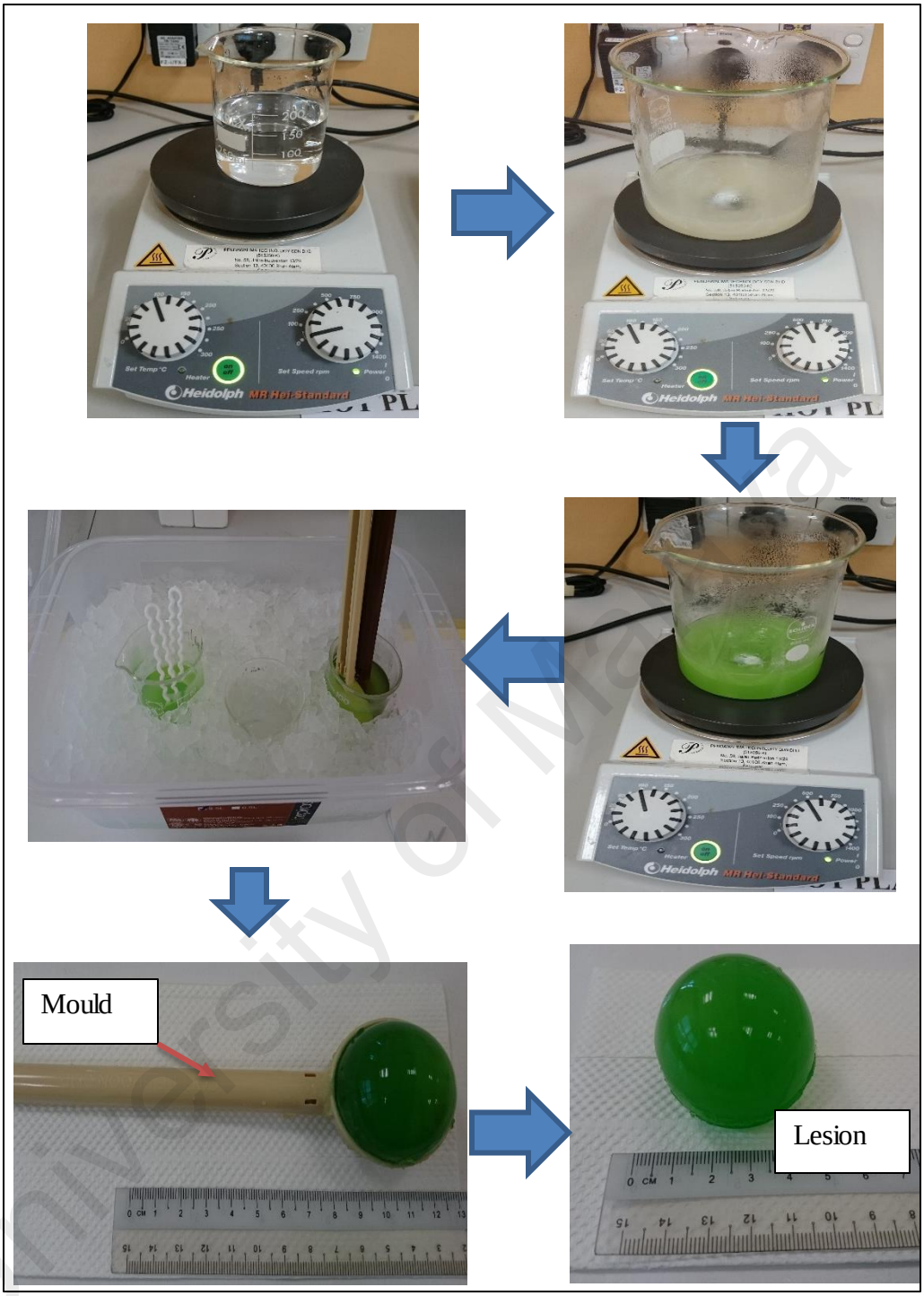

Figure 3.3 Steps preparation of tissue phantom

3.3.2 Construction of Background Phantom

Background phantom is required to hold the spherical inclusion in place during ultrasound scanning. Three layers of different thickness phantoms were constructed and combined as background phantom. The step by step procedures were described as follows:

1. Step 1 to 7 in Methods 3.1.1 (Preparation and development of tissue phantom) were repeated by using different amount of gelatine and distilled water to 80 g and 800 ml respectively. In this steps, no food colouring was added during the construction of phantom background.
2. After the molten gelatine was cooled, it was poured into the food container as a first layer with a thickness of 2 cm. The layer was homogeneously spread to allow same thickness at all sides. The surface was cooled until it was hard enough to support the lesions.
3. After the first layer had gelatinized, the spherical inclusions were placed and arranged on the top of the first layer according to the size and elasticity. Stickers were used to label the inclusion of different mass of gelatine.
4. Figure 3.3 showed second layer of molten gelatine was poured over the inclusion until it covered the small lesions (diameter 2.9 cm). The third layer was poured over the second layer and the remaining surface of the large lesions. For phantom at different depth, the third layer was measured at two different depth; 2 cm and 5 cm from the top surface of the large lesions respectively. Figure 3.5 and 3.6 showed the lesions at different depth. Each lesion was labelled on the surface of the container.
5. The phantom was kept in the chiller at a temperature of ~4°C for at least 1 hours until it was completely congealed.

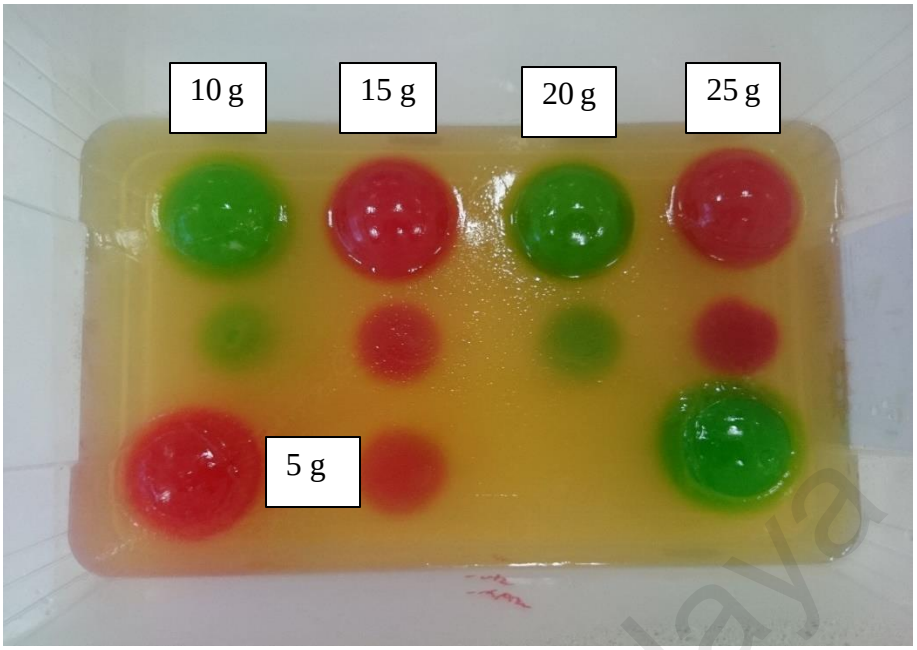

Figure 3.4 Arrangement of lesions in the background phantom

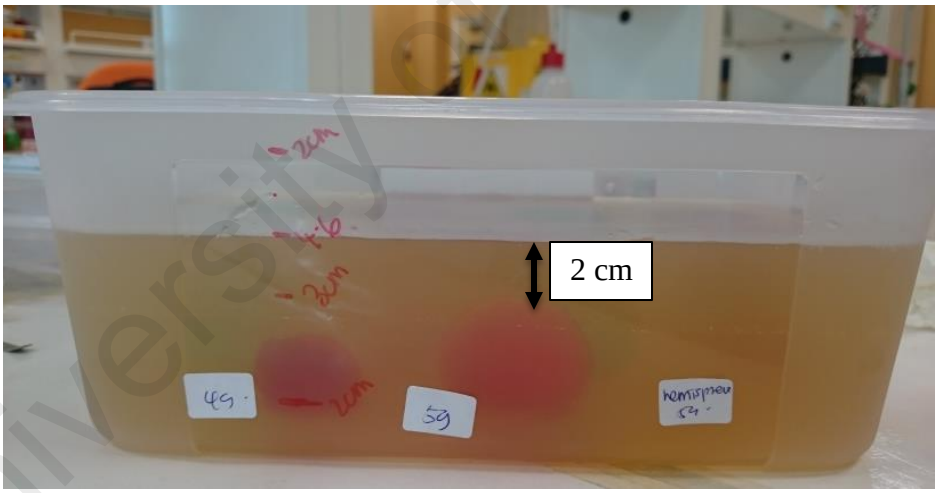

Figure 3.5 Side view of background phantom at 2 cm depth

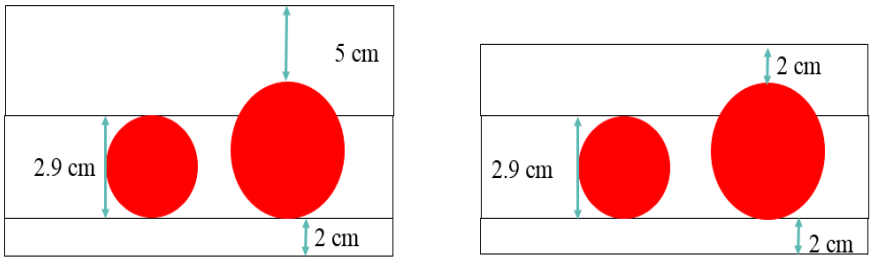

(a) (b)

Figure 3.6 Schematic diagram of phantom at 2 different depths **(a)** 5 cm and **(b)** 2 cm depth respectively.

3.3.3 Measurement of Tissue Elasticity

The stiffness of tissue phantoms constructed were measured by using shear wave imaging modalities; Ultrasound (Philips and Supersonic), Fibroscan® and Instron machines as a gold standard. All procedures in each machine was repeated three times and the mean elasticity (kPa) of each modalities was presented in graphical for in chapter 4.

3.3.3.1 Measurements using SWE Ultrasound, Philips

(a) (b)

Figure 3.7 (a) SWE Philips Ultrasound **(b)** 1.0 cm x 1.5 cm SWE box selected on ROI of the lesion. The image shows the elasticity, type of probe and frequency used.

The elasticity of tissue phantoms were measured using a SWE ultrasound system. The phantoms were scanned with a frequency of 22 Hz and curvilinear-array (C5-12) transducer was used for both grey-scale ultrasound and SWE (Lee *et al.*, 2012). Sky gel was applied on the surface of the phantom before the scanning started. To avoid cavitation, the amount of time that probe should be in contact with the phantom at a stationary position must be less than 20 seconds (Jaffaray, D. A., 2015).

Before the SWE measurement was measured, a B-mode (brightness mode) image was first obtained to visualize a portion of the phantom (Paparo *et al.,* 2013 & Yeong *et al.,* 2015). B-mode simultaneously scanned a plane through the phantom that can be viewed as 2D image on screen monitor. During the measurement of SWE, the transducer was statically held for a few seconds to obtain a stable image (Lee *et al.,* 2012). Lesions were compressed at the region of interest (ROI) to maximize the local displacement of lesion via acoustic pressure (Chang *et al.,* 2011).

Figure 3.7b showed SWE box (1.0 cm x 1.5 cm) was dragged on the lesion and the ROI was selected. Only one measurement of elasticity and velocity of the lesion can be obtained from one image. Mean and standard deviation of the elasticity and velocity of the lesions were obtained from at least three images of the ROI selected (top, middle and bottom) and the values were tabulated on Table 4.1- 4.4. The measurement using ultrasound Philips was performed by two operator; radiologist and sonographer. All images were saved and viewed using Q-Vue 1.1 software provided by Philips.

3.3.3.2 Measurements using SWE Supersonic Imagine

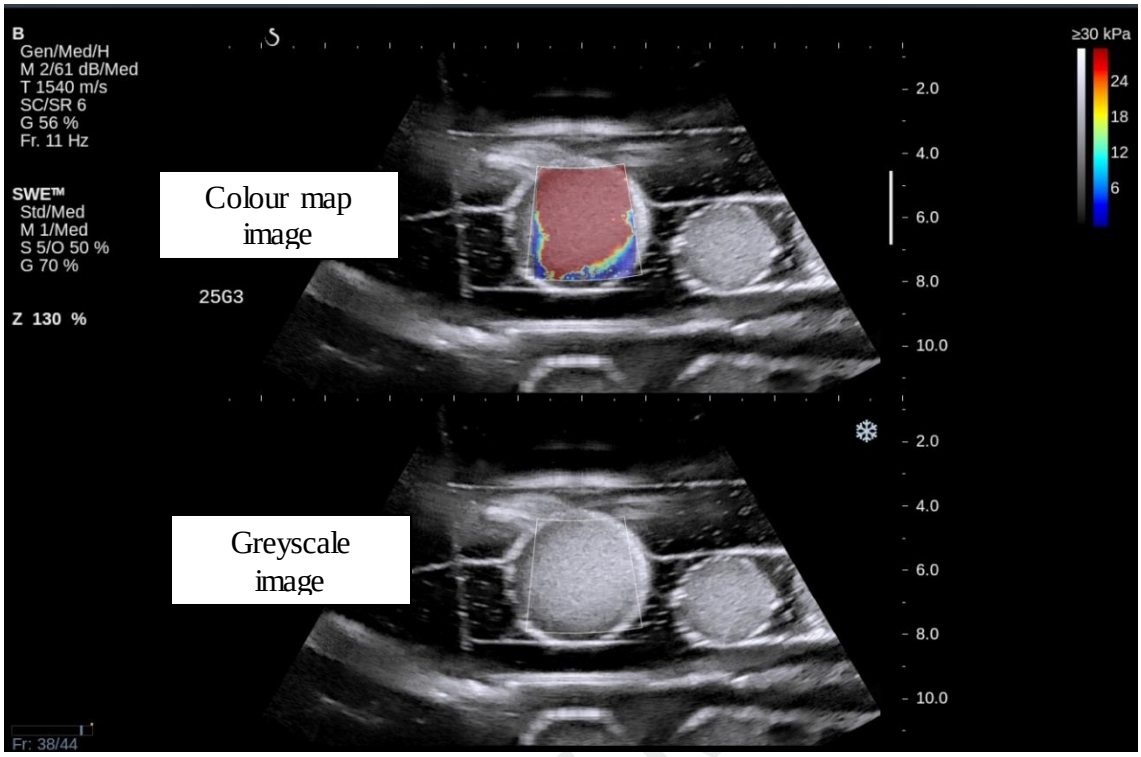

Figure 3.8 SWE box was resized according to the lesion size. Two images of greyscale and colour map were viewed at the same time.

The frequency, axial and lateral resolution was set to a range of about 7.5 to 15 MHz, 0.3 to 0.5 mm and 0.3 to 0.6 mm respectively (Yeong *et al.*, 2015). The ultrasound system was set to "Phantom" mode in the "General" application. As the probe was held stationary for a few seconds, the image on the monitor was freezed and two images which are the greyscale and the colour map images were obtained. Figure 3.8 showed the SWE box was dragged, resized and fitted according to the size of the lesion. As the colour map become homogeneous, three Q-box (ROI) were selected on the image. The information about the mean, minimum, maximum and standard deviation of the lesion can be obtained from the colour map image that was produced by the system (Lee *et al.*, 2012). Based on figure 3.8, Ooi *et al.* (2013) stated that, the colour map determines the hardness of the lesion; red colour represents high elasticity (>30kPa), green/yellow colour represents intermediate hardness and blue colour indicates softest/low elasticity.

3.3.3.3 Measurements using Fibroscan®

In Fibroscan, transient elastography technique was applied by using a low frequency (50 Hz) that was transmitted from the probe across the lesions (Paparo *et al.,* 2013). The probe used in the Fibroscan® is different from the ultrasound's probe. The tip of the probe is smaller and narrower and can easily break the surface of the phantom. Therefore, a 1.0 cm bolus was used and placed on the surface of the phantom before scanning. A drop of gel was placed on the tip of the E^+ probe to ensure suitable propagation of the ultrasonic signals. As the probe was placed perpendicular to the phantom, the pressure applied was monitored on the screen of the fibroscan (Wilder & Patel, 2014). The LEDs on the probe was on when the pressure was suitable enough to trigger the measurement and 10 successive measurements of the same lesion were obtained. Both results of controlled attenuation parameter (CAP) and stiffness values were displayed on the screen (Poynard *et al*., 2016).

3.3.3.4 Measurements using Instron 5969 (Gold Standard)

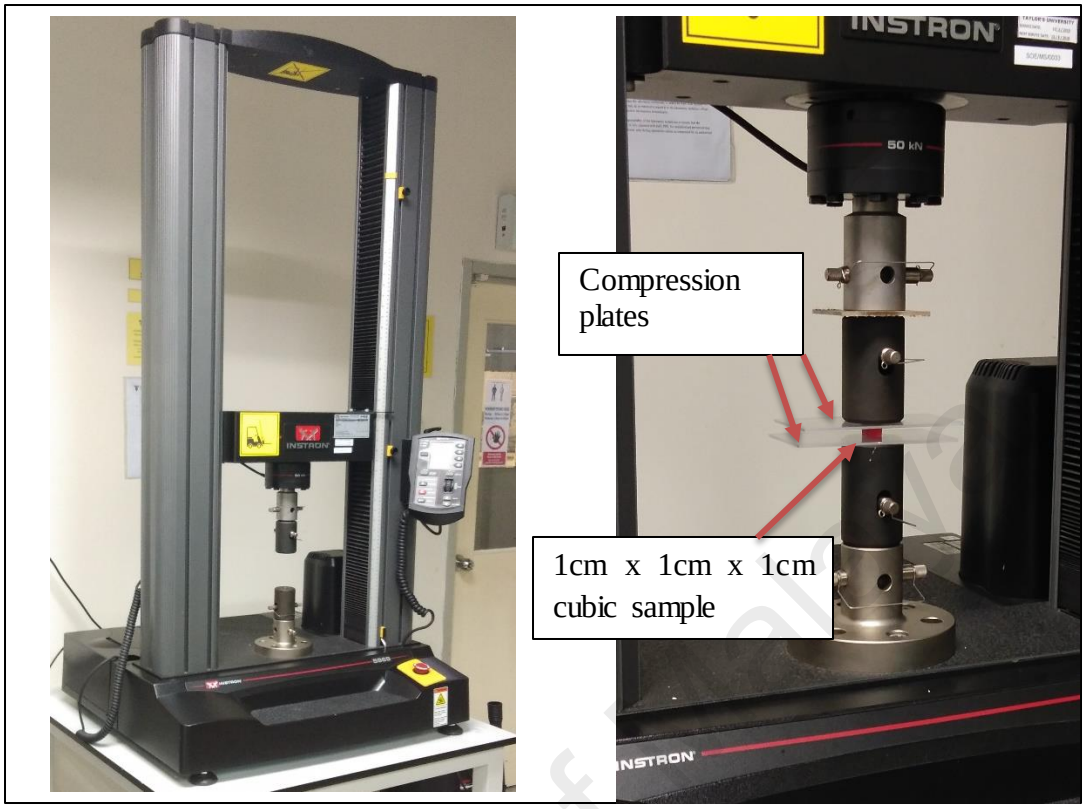

Figure 3.9 Sample was compressed between compression two plates

Instron 5969 tensile machine was used to measure the elasticity of the lesions which was deemed as a gold standard and compared with the elasticity measured using Fibraoscan and Ultrasound (Philips and Supersonic). Gold standard was measured to determine the likely of it with other test. This invasive method was performed by placing the sample in between two compressive plate.

As the position of spherical sample was hard to maintain and the non-uniformity shape will affect the stress applied onto the sample, the spherical inclusions of different masses were cut into 1 cm x 1 cm x 1cm cubical shape. Next, the load and displacement control rate for the compressive test was changed and set to 5kN and 0.5 mm/min respectively and graph of stress (kPa) vs. strain (mm/mm) was obtained from the Bluehills software. Figure 3.9 showed the sample was placed in between two compressive plate and this test was immediately stopped after the sample was totally destroyed and the graph of stress

vs. strain deformed. Young's modulus of each sample of different mass of gelatine can be obtained from the slope of the stress vs. strain graph.

3.3.4 Comparison of Shear Wave Imaging (Philips, Supersonics and Fibroscan®) and Gold Standard (Instron™)

Each elasticity value obtained from each modality was tabulated and presented in graphical form. The graphs were observed and compared for statistical analysis.

CHAPTER 4: RESULTS AND DISCUSSION

4.1 2D Shear wave Ultrasound Elastography (iU22, Philips, USA)

Figure 4.1 – 4.5 show images of lesion of different elasticity scanned using ultrasound SWE, Philips. Average elasticity and velocity of both 2.9 cm and 4.5 cm diameter lesions were obtained by measuring at least at three different area.

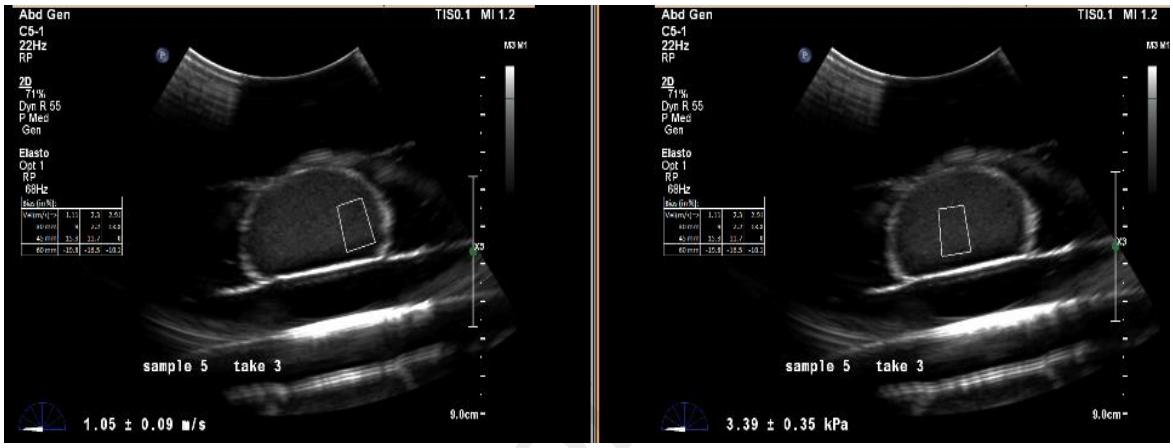

Figure 4.1 Elasticity and velocity measured on lesion of 5 g of gelatine

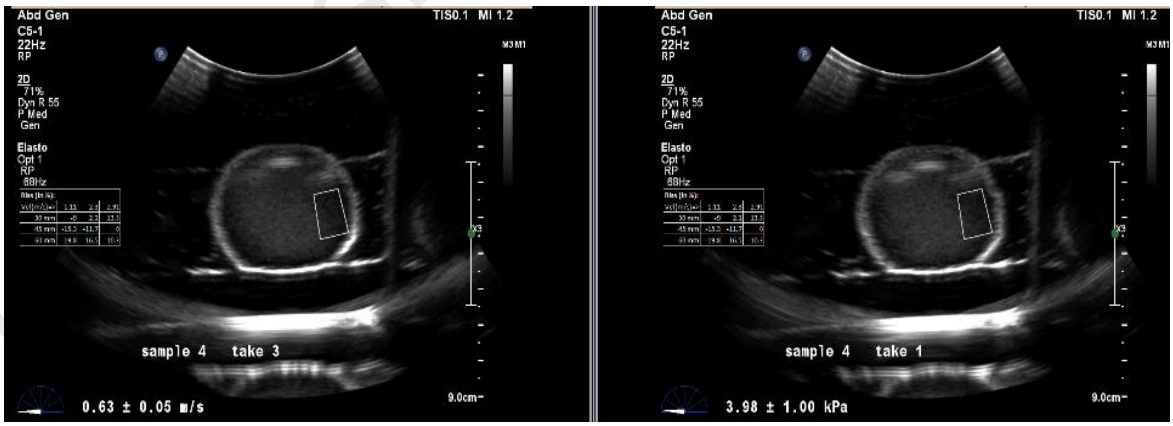

Figure 4.2 Elasticity and velocity measured on lesion of 10 g of gelatine

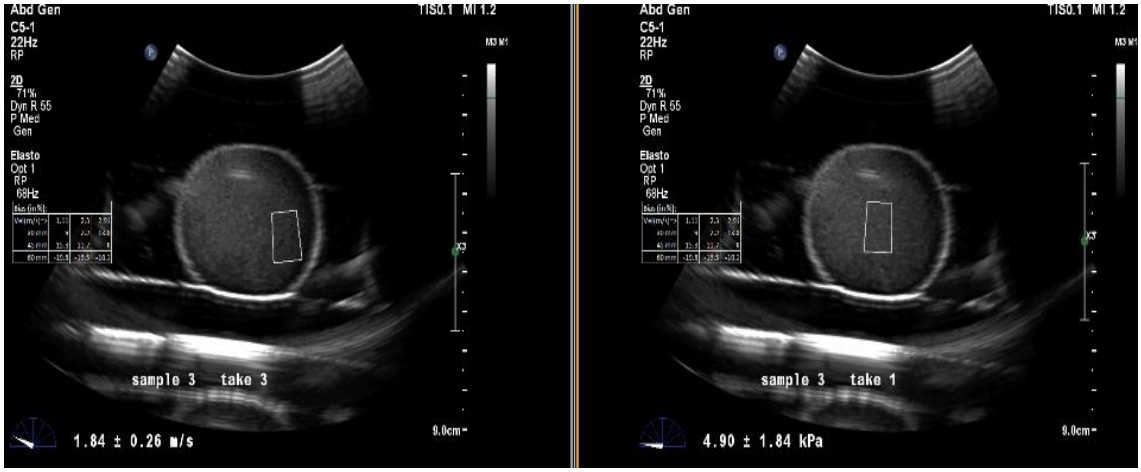

Figure 4.3 Elasticity and velocity measured on lesion of 15 g of gelatine

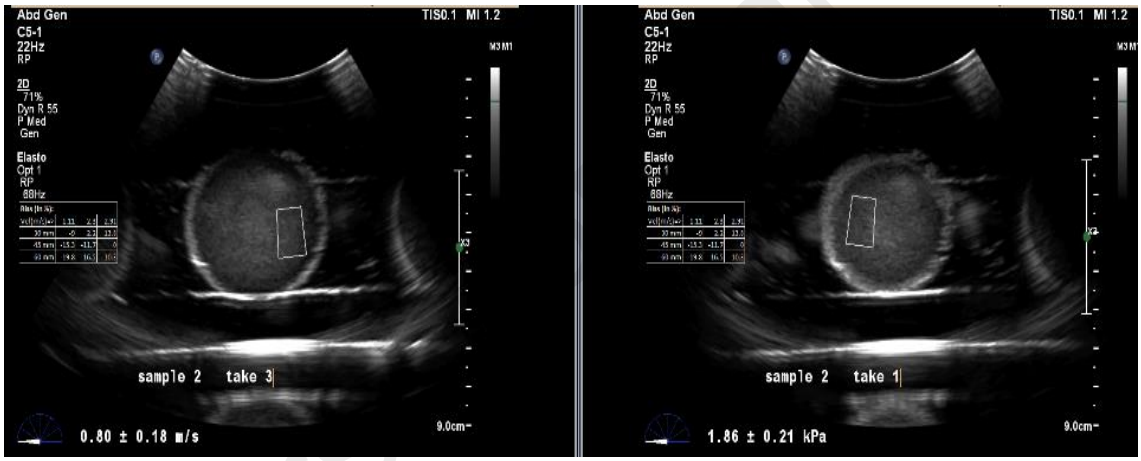

Figure 4.4 Elasticity and velocity measured on lesion of 20 g of gelatine

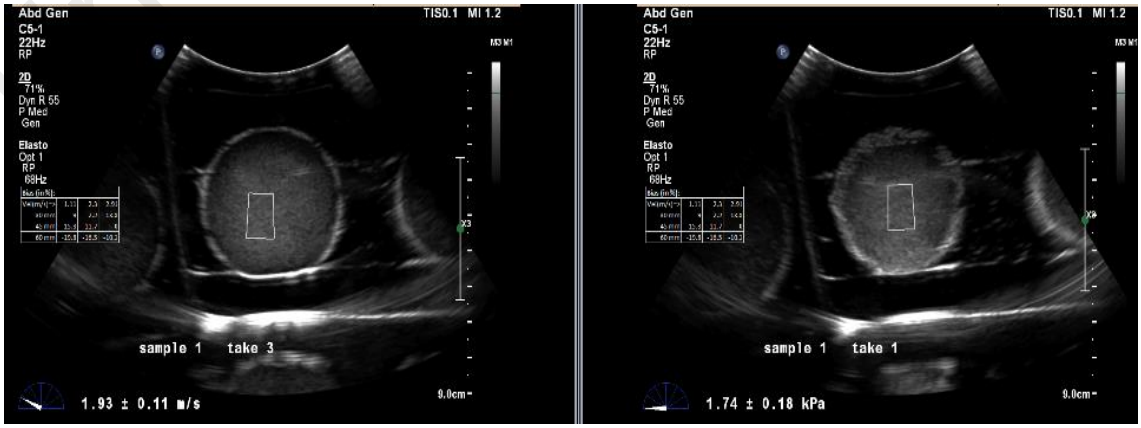

Figure 4.5 Elasticity and velocity measured on lesion of 25 g of gelatine

Table 4.1 and 4.2 show the mean results of elasticity and velocity measured at two different depth from the surface. These results were obtained from two operators, table 4.1 and 4.2 were both observed by a radiologist and sonographer. Data shown were average of three ROI selected from each lesion. Figure 4.6 and 4.7 show graph of elasticity meanwhile figure 4.8 and 4.9 show graph of velocity observed by (a) operator A and (b) operator B at two different depth from the surface.

Table 4.1 Mean elasticity and velocity at depth of 2 cm from the surface

Size (cm)	Mass of Gelatine (g)	Radiologist		Sonographer	
		Velocity (m/s)	Elasticity (kPa)	Velocity (m/s)	Elasticity (kPa)
4.5	5	1.16 ± 0.10	4.04 ± 0.72	0.92 ± 0.02	2.52 ± 0.09
	10	1.77 ± 0.24	9.41 ± 2.55	1.51 ± 0.12	6.88 ± 1.05
	15	3.09 ± 0.20	28.66 ± 3.58	2.78 ± 0.20	23.19 ± 3.22
	20	1.70 ± 0.24	8.63 ± 2.43	3.30 ± 0.26	32.64 ± 5.05
	25	3.10 ± 0.46	28.76 ± 8.11	5.90 ± 0.14	104.28 ± 4.86
2.9	5	1.25 ± 0.32	2.45 ± 0.64	1.31 ± 0.20	5.11 ± 1.47
	10	1.45 ± 0.27	9.18 ± 2.55	1.85 ± 0.14	10.24 ± 1.56
	15	1.75 ± 1.7	12.39 ± 4.90	3.18 ± 0.15	30.31 ± 2.73
	20	2.43 ± 0.18	4.05 ± 2.63	1.38 ± 0.23	5.71 ± 1.88
	25	1.44 ± 0.84	4.09 ± 1.07	5.43 ± 0.59	88.33 ± 17.88

Table 4.2 Mean elasticity and velocity at depth of 5 cm from the surface

Size (cm)	Mass of Gelatine (g)	Radiologist		Sonographer	
		Velocity (m/s)	Elasticity (kPa)	Velocity (m/s)	Elasticity (kPa)
4.5	5	1.25 ± 0.1	3.37 ± 1.34	1.04 ± 0.72	1.16 ± 0.10
	10	2.43 ± 0.03	21.71 ± 3.91	1.77 ± 0.24	9.41 ± 2.55
	15	1.00 ± 0.25	3.07 ± 1.70	3.09 ± 0.20	28.66 ± 3.58
	20	1.12 ± 0.52	5.07 ± 2.40	1.70 ± 0.24	8.63 ± 2.43
	25	1.77 ± 0.07	5.63 ±1.53	3.10 ± 0.46	28.76 ± 8.11
2.9	5	0.97 ± 0.03	2.86 ± 1.00	0.90 ± 0.12	2.45 ± 0.64
	10	1.89 ± 0.50	6.37 ± 2.45	1.75 ± 0.25	9.18 ± 2.55
	15	1.21 ± 0.08	3.49 ± 1.41	2.03 ± 0.44	12.39 ± 4.90
	20	1.35 ± 0.16	5.81 ± 3.15	1.16 ± 0.39	4.05 ± 2.63
	25	1.43 ± 0.02	4.35 ± 1.01	1.17 ± 0.15	4.09 ± 1.07

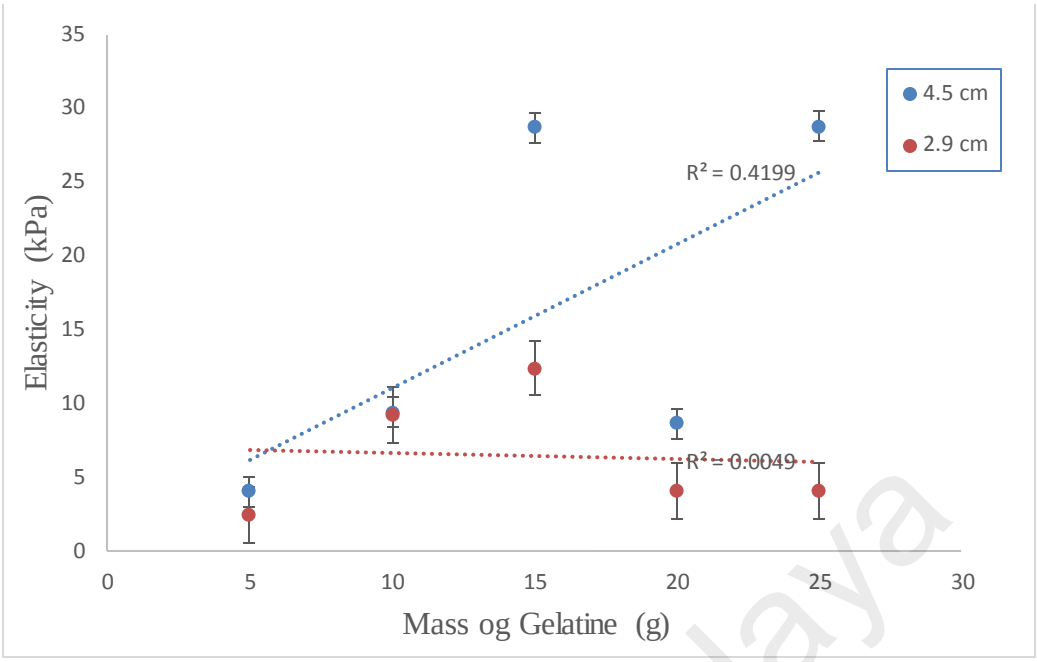

(a)

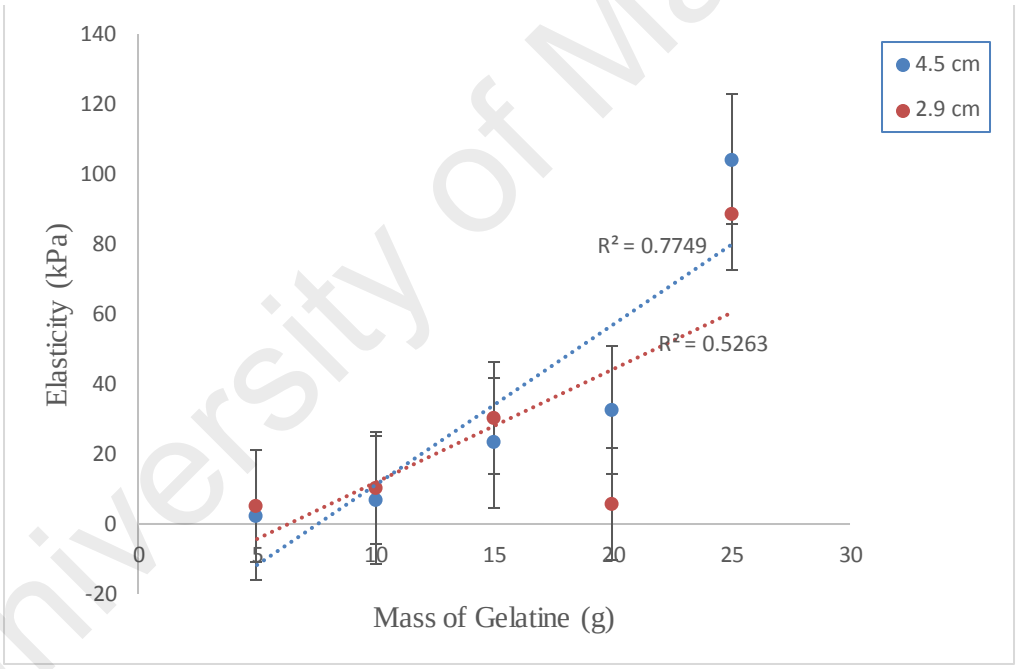

(b)

Figure 4.6 Graph of comparison between the elasticity values of inclusions of two different sizes at a depth of 2 cm from the surface **(a)** radiologist **(b)** sonographer.

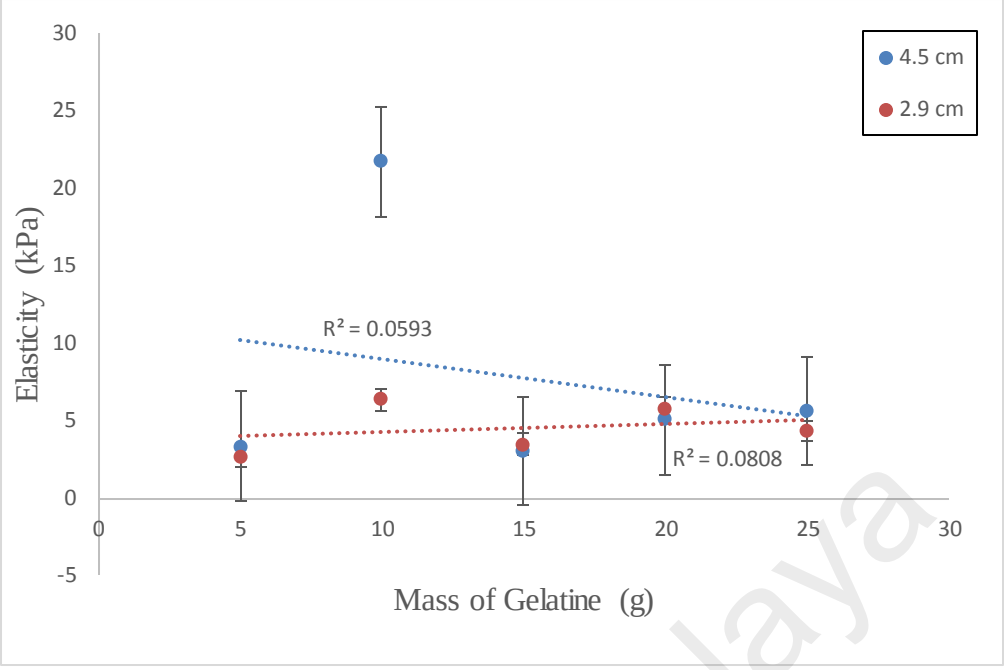

(a)

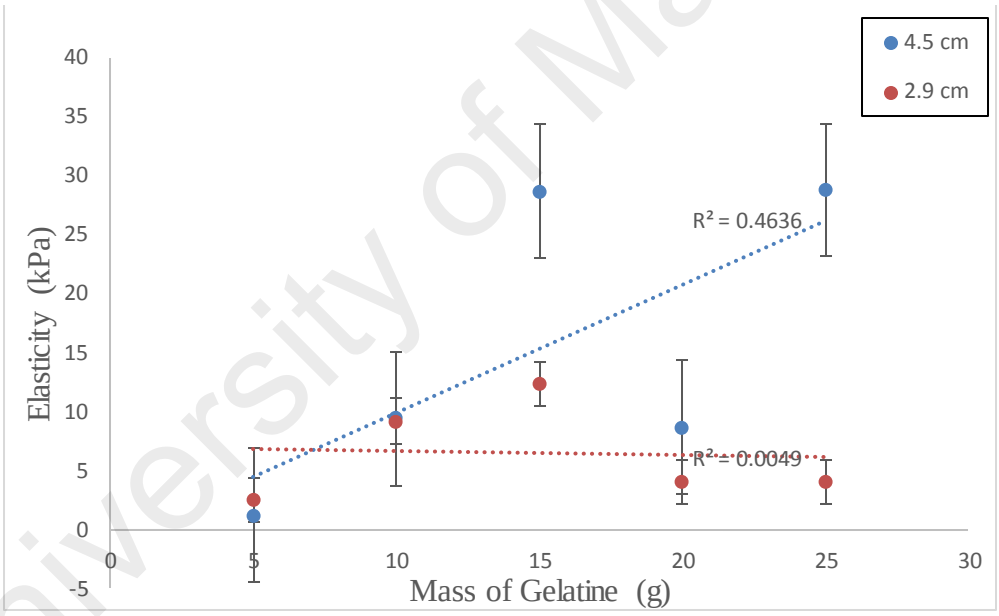

(b)

Figure 4.7 Graph of comparison between the elasticity values of inclusions of two different sizes at a depth of 5 cm from the surface **(a)** radiologist **(b)** sonographer.

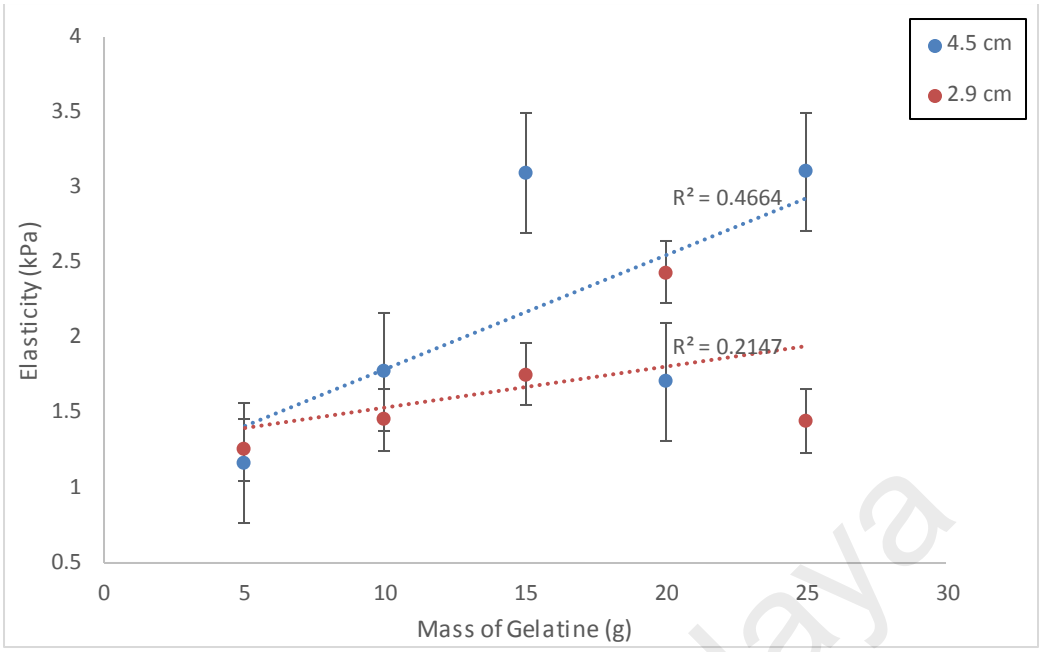

(a)

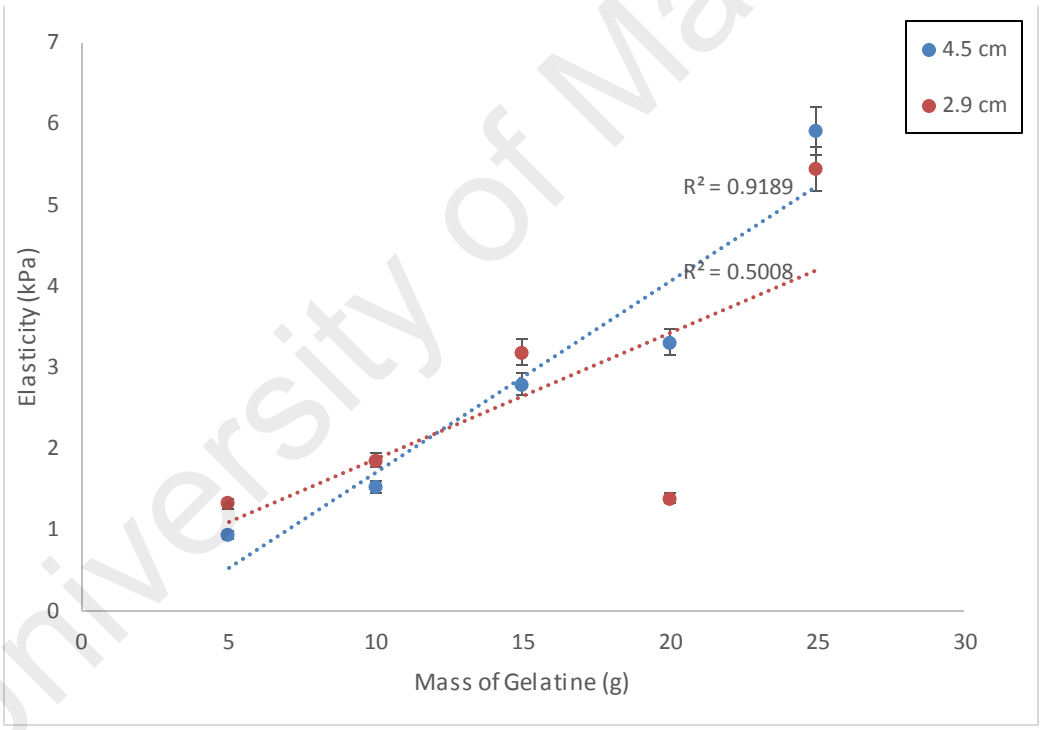

(b)

Figure 4.8 Graph of comparison between the velocity values of inclusions of two different sizes at a depth of 2 cm from the surface **(a)** radiologist **(b)** sonographer.

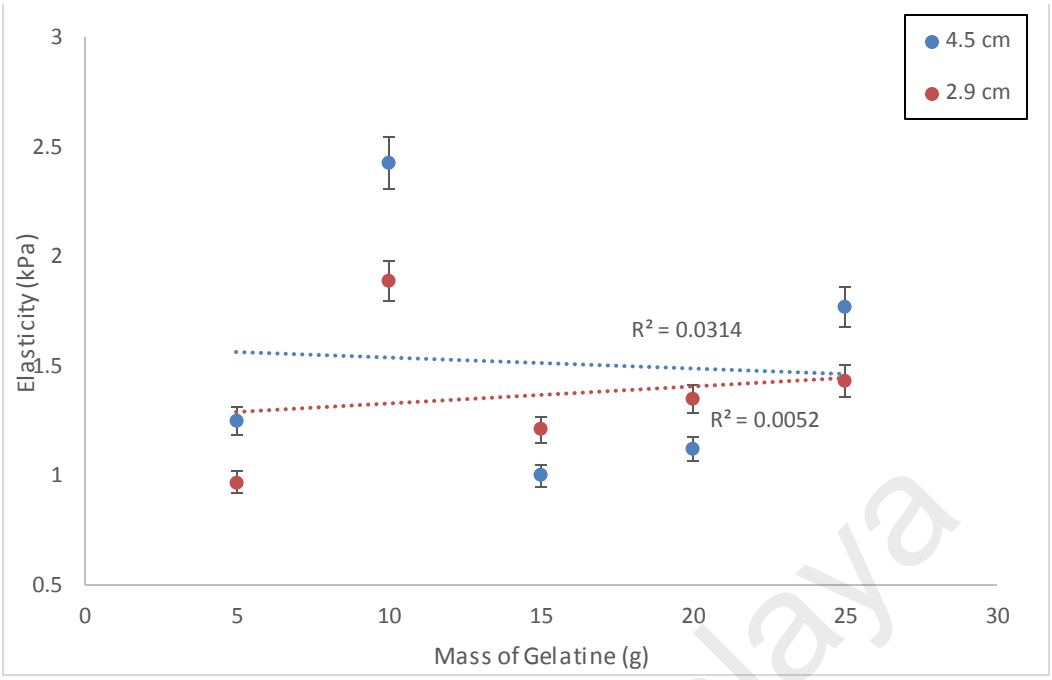

(a)

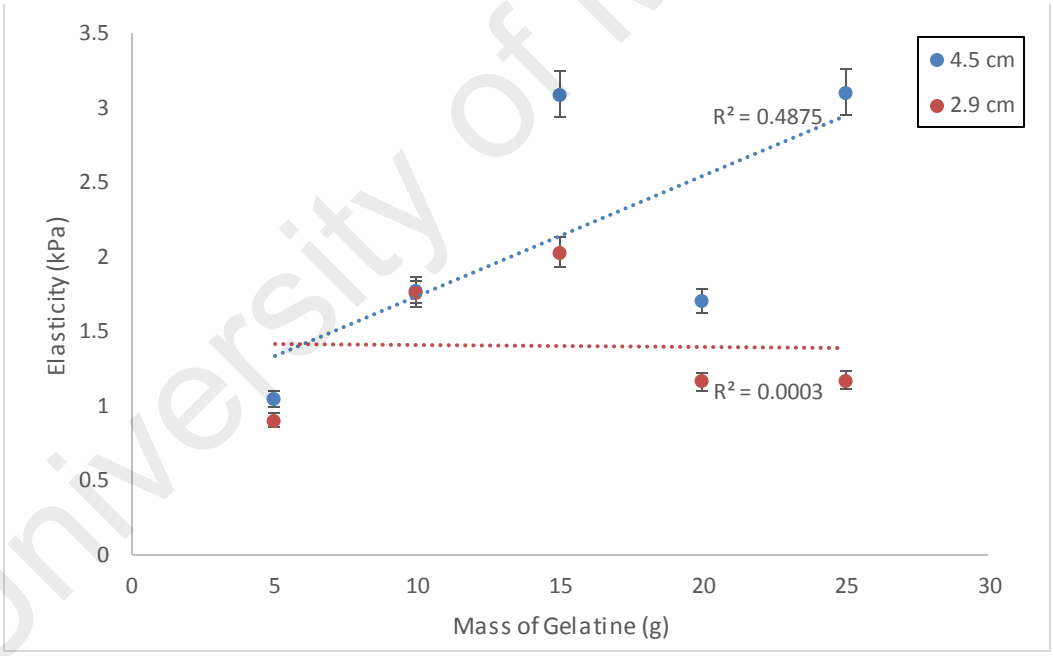

(b)

Figure 4.9 Graph of comparison between the velocity values of inclusions of two different sizes at a depth of 5 cm from the surface **(a)** radiologist **(b)** sonographer.

Since the elasticity and velocity of the lesion was examined by two operators, the mean values were compared between subject groups also using the paired *t*-test (two-tailed) at 0.05 significance level (α=0.05). According to Lee *et al.* (2012), the higher the elasticity of the lesion/tissue, the velocity of SWE propagate through it is higher and the elasticity was supposed to increase at high tissue/lesion composition. In this observation only figured 4.6b and 4.8b which was examined by the sonographer showed a positive r^2 value in elasticity when the mass of gelatine increased. Figure 4.6b and 4.8b show that at a depth of 2 cm from the surface, the elasticity and velocity of SWE increase as the mass of lesion with 4.5 cm increased. Among these results, SWE propagates better when the size of lesion is bigger and depth of lesions were closer to the surface.

Table 4.3 Results of paired *t*-test of mean elasticity and velocity made by radiologist and sonographer.

	Depth from surface (cm)	P-value	Conclusion
Elasticity (kPa)	2	0.305	No significant difference
	5	0.250	
Velocity (m/s)	2	0.360	
	5	0.376	

Based on table 4.3, the results of paired *t*-test showed that mean difference of elasticity and velocity showed no significant different when compared with p-value ($p>0.05$). This means that the results observed by both radiologist and sonographer showed no different and the mean observed by both were almost the same.

4.2 2D Shear wave Ultrasound Elastography (Aixplorer V6, Supersonic Imagine, France)

Figure 4.10- 4.14 show images of lesion of different elasticity scanned using ultrasound Supersonic. Image can be viewed in two form; greyscale and colour coded image. The lesions were mixed well and homogeneous based on the colour showed on the images. The red colour indicates that the lesion hardness is high (≥30 kPa) meanwhile the blue colour indicates that the hardess is low (≤ 6 kPa) (Leschied, 2014). This indication is stated on the image monitor during scanning. SWE Supersonic only measured the hardness of the lesion therefore the velocity of the wave travel through the lesion cannot be determined and the velocity assumed by the machine was 1540 m/s. Due to time limitation, only one operator (radiologist) managed to examine the elasticity using ultrasound Supersonics.

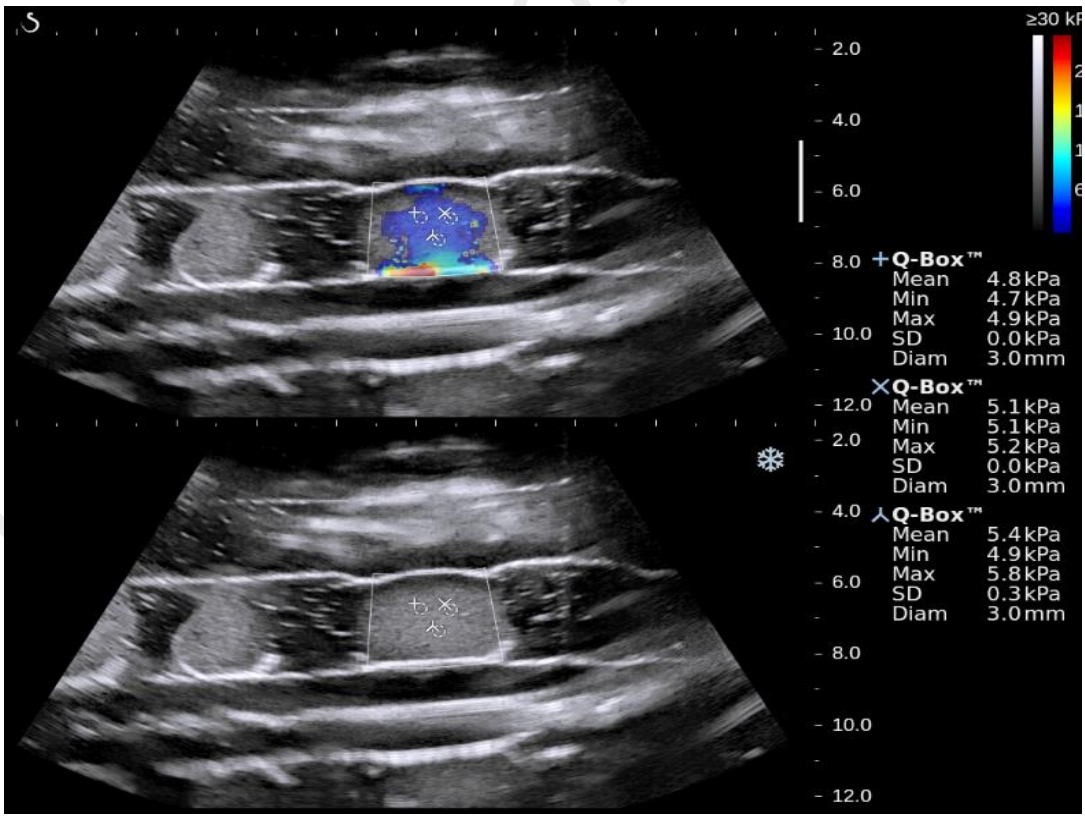

Figure 4.10 Elasticity measured using SWE mode on 5 g of gelatine

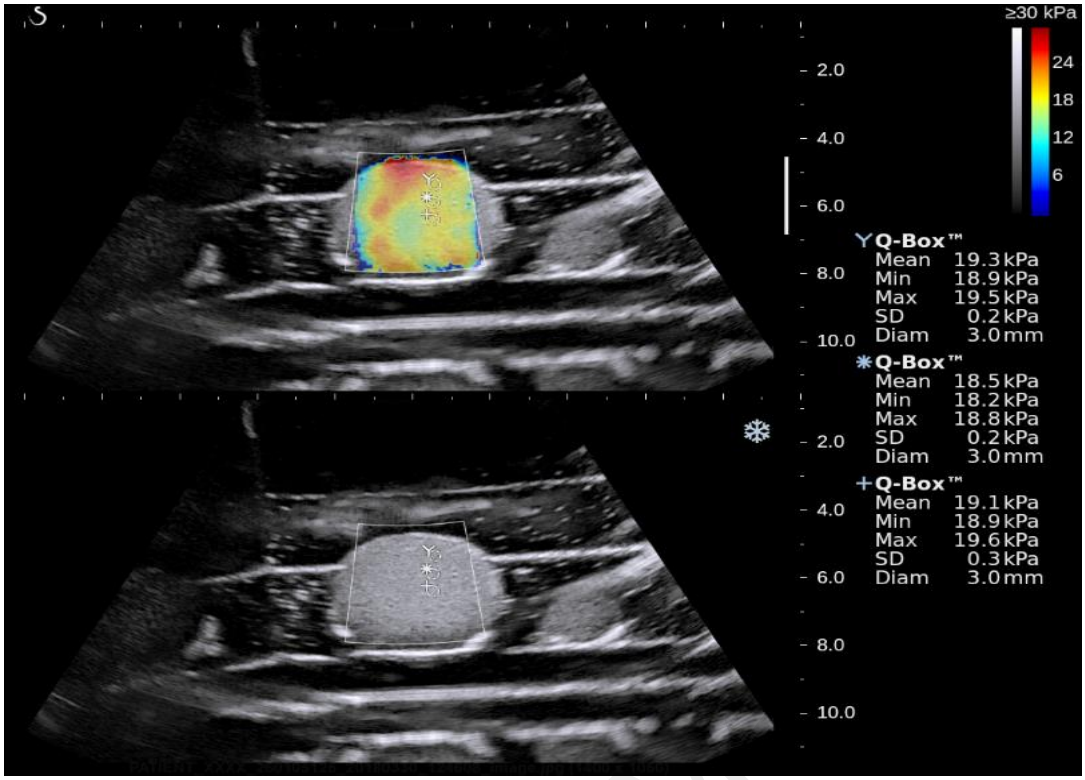

Figure 4.11 Elasticity measured using SWE mode on 10 g of gelatine

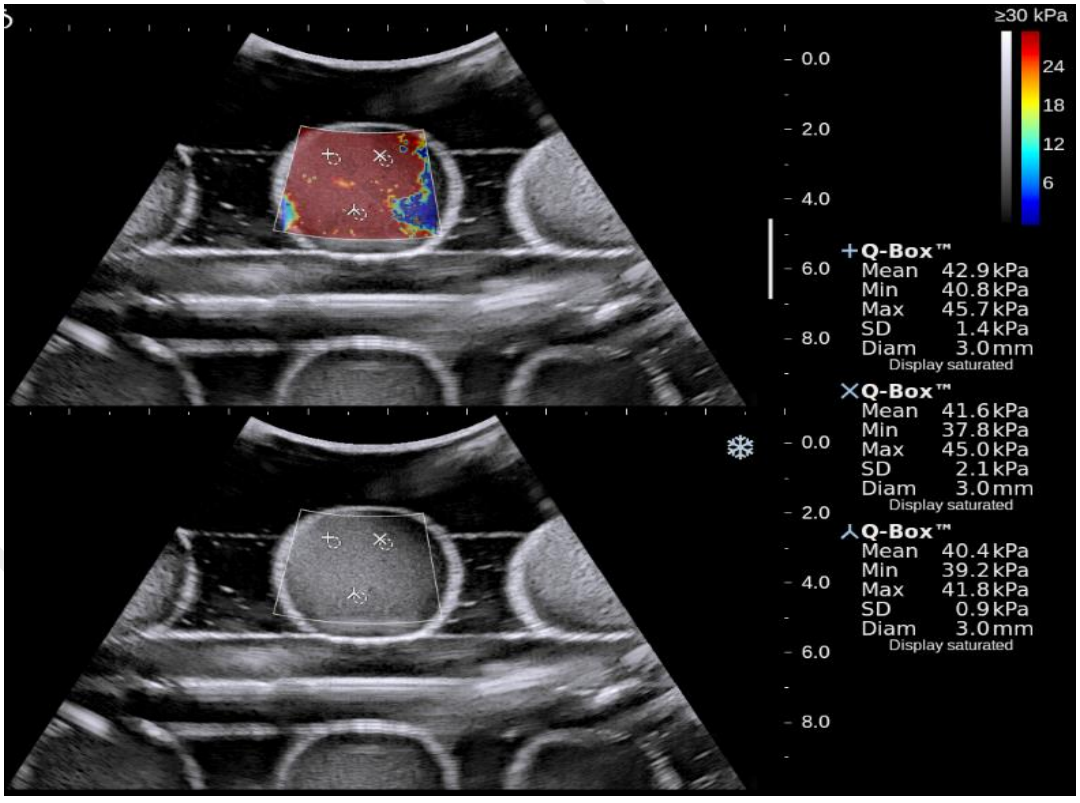

Figure 4.12 Elasticity measured using SWE mode on 15 g of gelatine

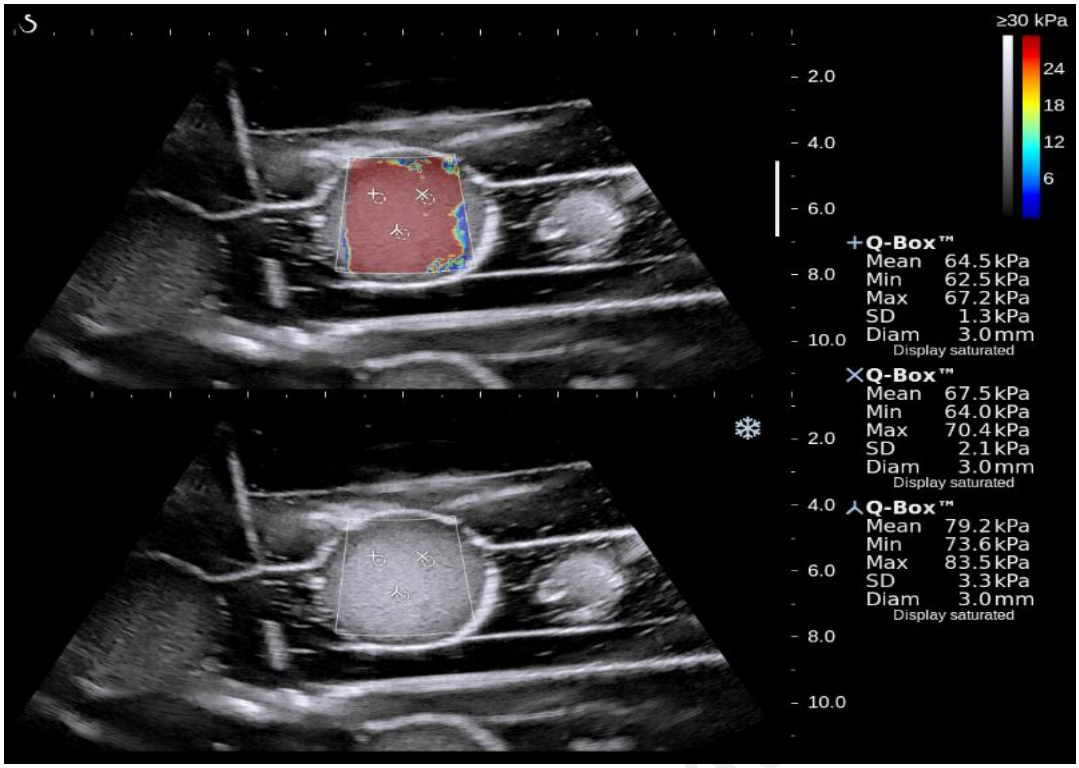

Figure 4.13 Elasticity measured using SWE mode on 20 g of gelatine

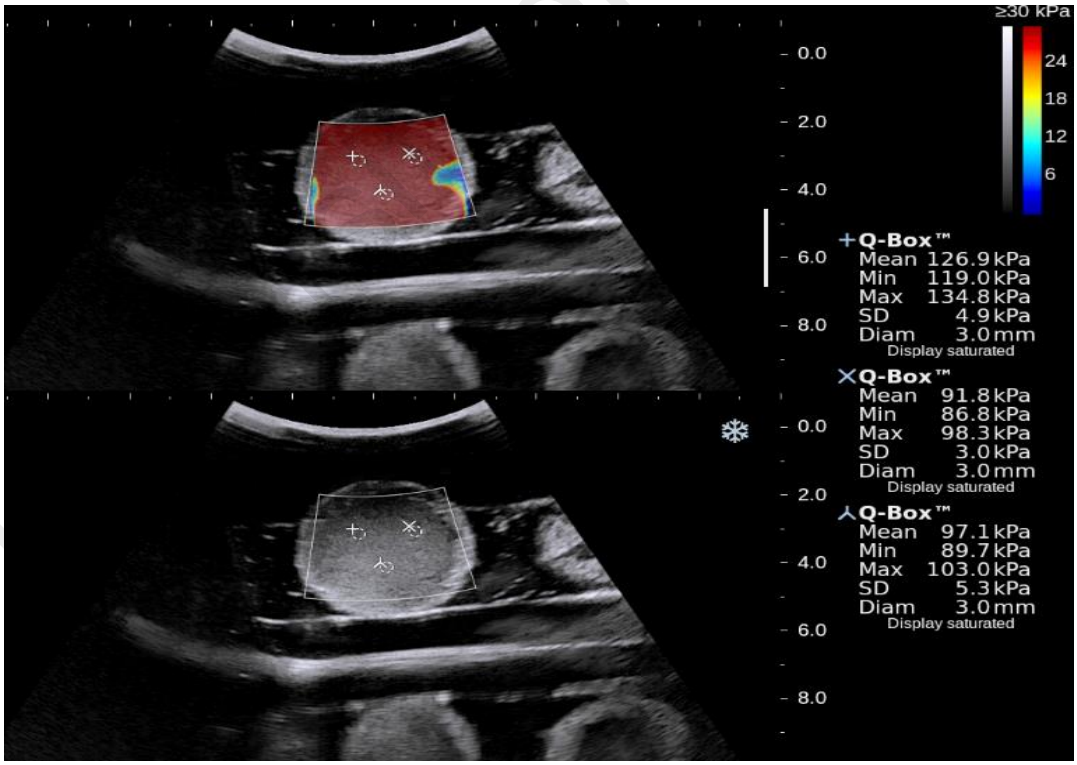

Figure 4.14 Elasticity measured using SWE mode on 25 g of gelatine

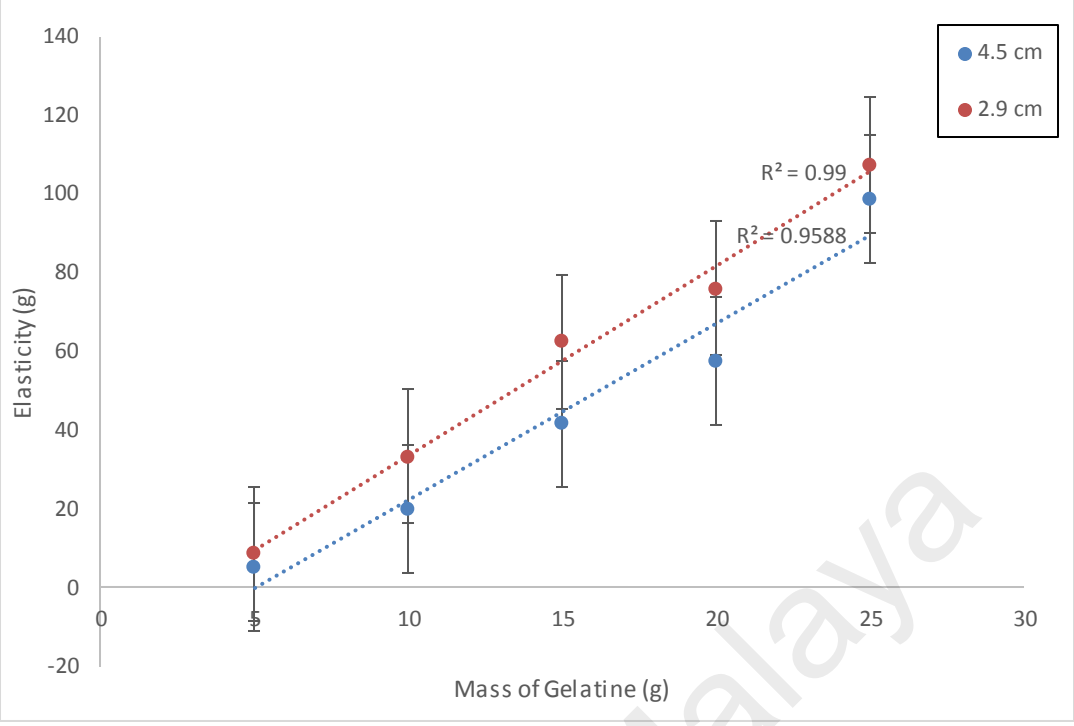

Figure 4.15 Graph of comparison between the elasticity values of inclusions of two different sizes at a depth of 2 cm from the surface.

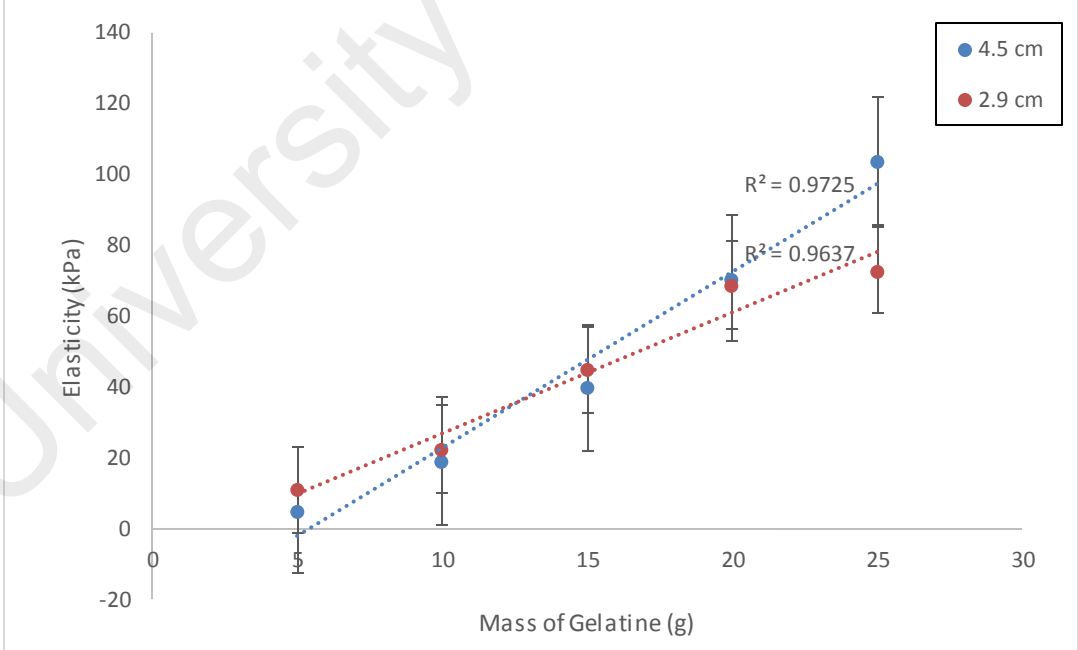

Figure 4.16 Graph of comparison between the elasticity values of inclusions of two different sizes at a depth of 5 cm from the surface.

Figure 4.15 and 4.16 show graph of comparison of elasticity of lesion at two different depth; 2 cm and 5 cm respectively. The elasticity of the lesion increased as the mass of gelatine increased. The Pearson's r at 2 cm is 0.99 and at 5 cm is 0.96 meanwhile the r^2 values at these depth were 0.97 and 0.96 respectively. These results showed that the elasticity have strong correlation by the change of mass of gelatine compared to the correlation obtained from US Philips.

4.3 1D Transient Elastography (Fibroscan®)

During first measurement, the scanning was failed because the phantom was perforated and destroyed due to the narrow tip of the probe. Therefore on second scanning, a 1.0 cm bolus was placed on the surface of the phantom, without bolus the narrow tip of the probe will perforated the surface of the phantom again. A bolus was used due to its tissue equivalent characteristics. Figure 4.17 shows the image of Fibroscan® Echosens™ monitor screen during examination. 10 measurements was conducted on both phantom, however none of these measurements were valid. According to Echosense (2018), the $^{+}$E (medium) probe can measured from 25 mm up to 65 mm below the skin to capsule distance (depth) and the depth of penetration for the XL^{+} (large) probe is 35 mm to 75 mm. Even after the probe was changed from $^{+}$E to XL^{+} and a suitable pressure was applied the monitor still showed invalid measurement. The depth of lesions from the surface for first phantom was 2 cm and the second phantom was 5 cm which was within the skin to capsule distance for the transient elastography wave to pass through the lesion for both types of probe. Although the positioning of the probe was already perpendicular to the lesions but the elasticity still cannot be measured. However when a random examination was conducted on a volunteer named subject A, 10 valid measurements were obtained. Figure 4.18 shows results of both stiffness and controlled attenuation parameter (CAP) from the examination. Therefore due to this invalid measurement, no statistical analysis can be calculated and no comparison can be made from Fibroscan.

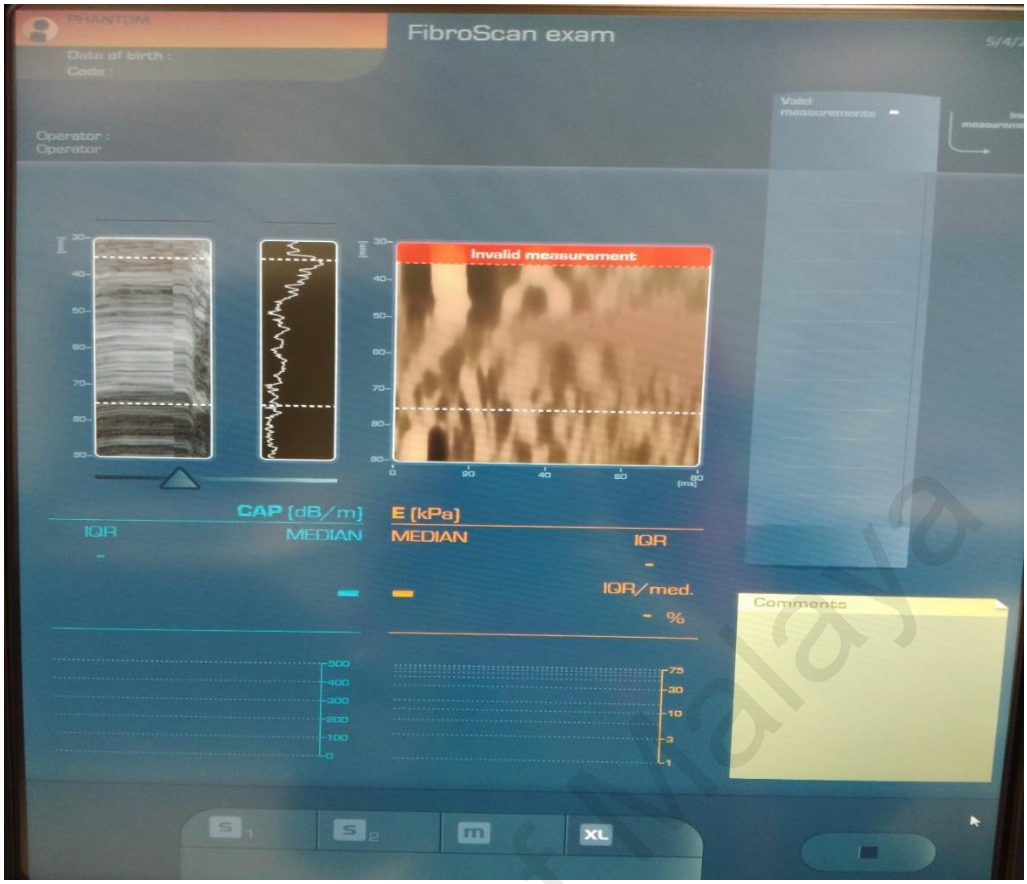

Figure 4.17 Invalid measurement during phantoms scanning using Fibroscan®

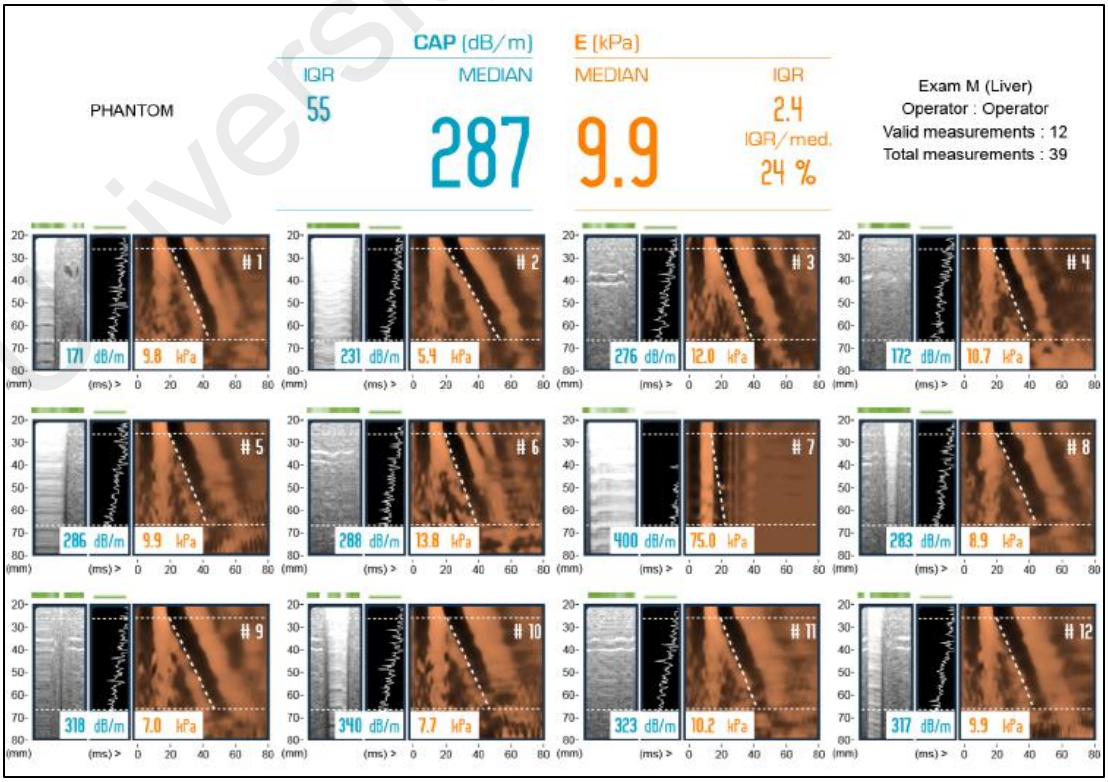

Figure 4.18 Fibroscan® results conducted on subject A (volunteer)

4.4 Tensile Machine (Instron , Gold Standard)

Figure 4.19 show graph of compressive stress vs. compressive strain using tensile testing machine Instron 5969. Based on equation (1), the graph of Young's modulus was obtained from the slope of theses graph and was used as a gold standard and compared with SWE Philips and Supersonics. As the sample was compressed at 5 kN, the graph increased but as sample deformed, the graph dropped. This indicate that the sample had reached its ultimate strength and deformed beyond the strength. Figure 4.20 shows graph of Young's modulus increase with increase of mass of gelatine..

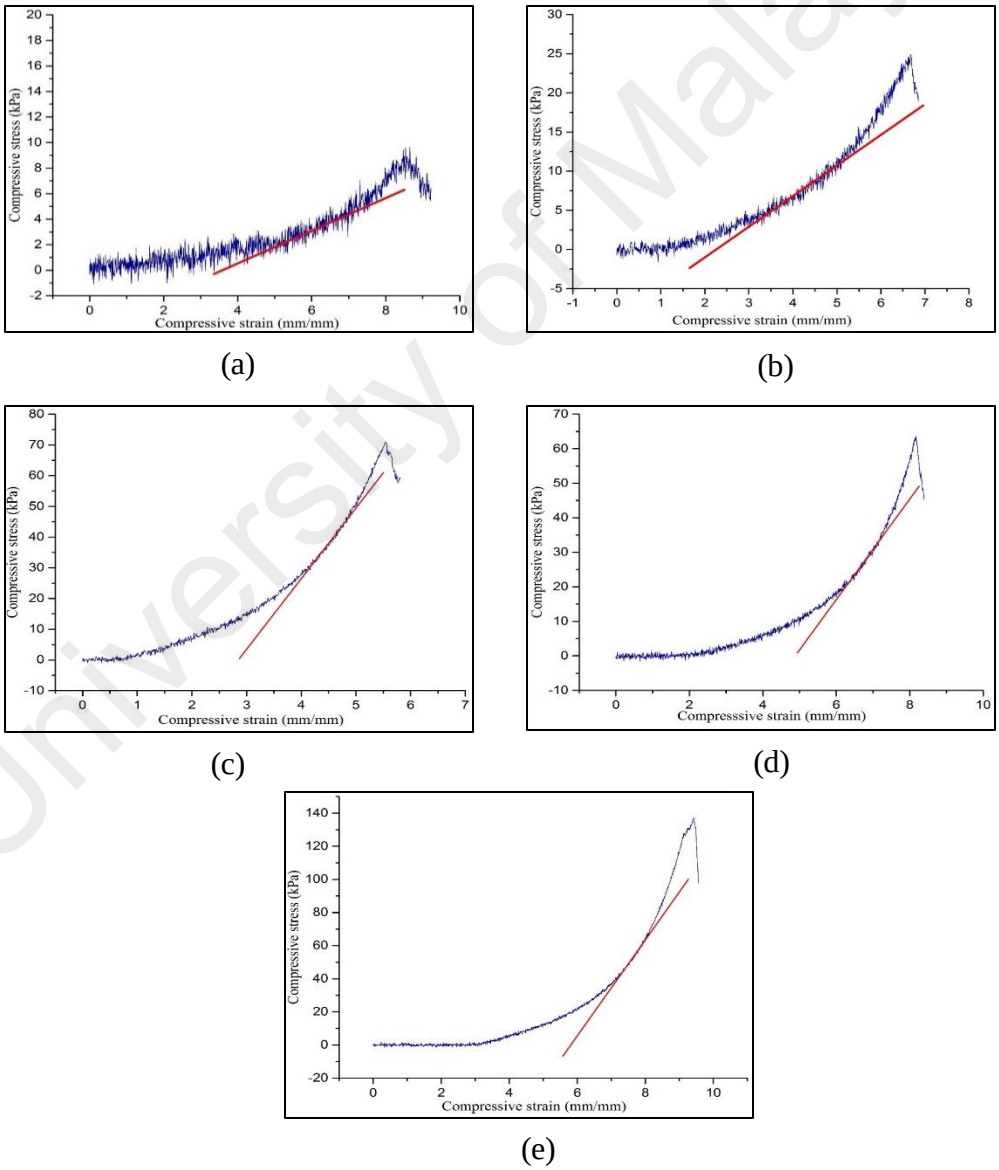

Figure 4.19 Graph of stress against strain for lesion of **(a)** 5 g, **(b)** 10 g, **(c)** 15 g, **(d)** 20 g and **(e)** 25 g of gelatine

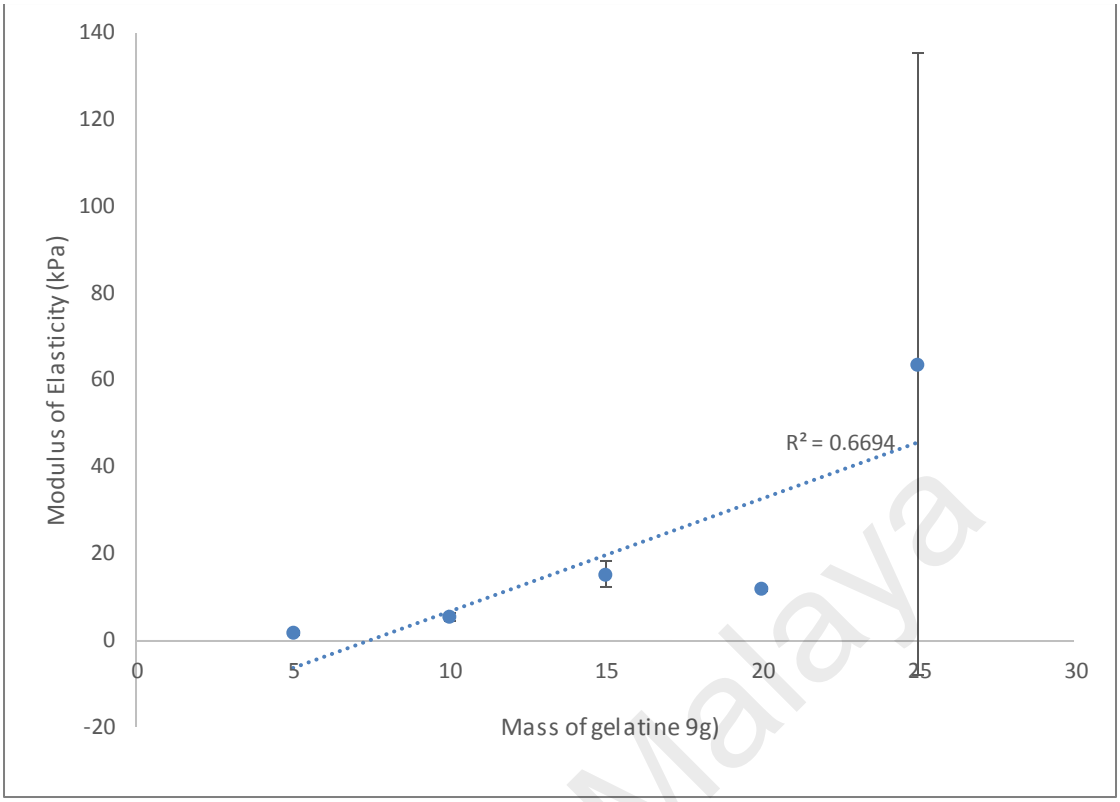

Figure 4.20 Graph of young modulus *vs.* mass of gelatine measured by Instron

4.5 Comparison of SWE and Gold Standard

During measurement of SWE, it was noticed that the values of elasticity measured for the same lesions were sometimes have a different for more than 10 kPa. This seemed to indicate that the lesion was not mixed well and not homogeneous. However when the lesion was viewed under ultrasound Supersonic Imagine colour map, colour in the range of elasticity was showed; red indicates high stiffness, yellow/green indicates intermediate stiffness and blue indicates low stiffness. This colour map helped to explain the homogeneity of the lesion, and based on figure 4.10-4.14, the mixture of gelatine and calcium carbonate is homogeneous. However, during SWE measurements, the elasticity values of the same lesion still varied from one another.

Table 4.4 Paired samples T-test of elasticity measurement between SWE modalities and Instron

	Parameters		Pair differences		P-values (0.05)
	Depth (cm)	Lesion size (cm)	Mean	Standard deviation	
US Philips - Instron	2	2.9	13.08	26.56	0.33
		4.5	3.61	19.38	0.70
	5	2.9	8.43	13.56	0.23
		4.5	14.39	16.27	0.11
US Supersonics-Instron	2	2.9	38.09	21.07	0.01
		4.5	25.11	15.74	0.39
	5	2.9	24.32	18.94	0.05
		4.5	28.03	20.59	0.04
US Philips - US Supersonics	2	2.9	51.17	38.41	0.04
		4.5	28.73	29.31	0.09
	5	2.9	39.29	27.04	0.03
		4.5	41.11	40.94	0.09

Table 4.4 shows the results obtained from the calculation of paired sample *t*-test for data sets measured using SWE (Philips and Supersonics) and Instron. Fibroscan® was excluded from these calculation and comparison since no data was obtained during scanning. Based on the results showed that only US Supersonics-Instron were significantly differ while the mean elasticity between US-Philips were statically no significant difference between the mean elasticity. As for US Philips, the mean elasticity measured by the radiologist was picked and standardize as other measurements were also performed by the same radiologist. The Pearson correlation (r) and regression (r^2) of SWE Supersonics-Instron measured were 0.94 and 0.85 respectively and this means that there exists strong relationship between elasticity and mass of gelatine within two machine. Mean elasticity between US Philips and US Supersonics were compared. Based on table 4.4, there was a significance different in mean elasticity for lesion with 2.9 cm diameter at both depth. The mean elasticity measured by Instron tensile machine as gold standard was smaller than the mean elasticity measure by both US Philips and US Supersonics, however the mean difference between US Supersonic and Instron was much greater and the values was overestimated by 5 to 44 kPa than its actual elasticity. According to Yeong

et al. (2015), this overestimation might due to the system assumption that all body and tissues have the same body density of 1 g cm^{-3}. However, human body are consist of different types of tissue and each tissue have different density. The phantom analysis showed that the inclusions were detected by all of the elastometry systems, even when it were poorly visualised in B mode and that they were better detected if they were harder (Franchi-Abella *et al.*, 2013).

Based on the mean elasticity results and figure 4.20, the difference in elasticity and Young's modulus measured by three modalities were due to some errors. Both US showed different elasticity although ROI was selected on the same area of the same lesions which lead to large range of elasticity measurements. Besides that, figure 4.20 showed one outlier at point 25 g of gelatine. The average modulus of elasticity calculated was much higher and the standard error obtained was also larger than others, therefore this point was considered as an outlier for Instron.

CHAPTER 5: LIMITATION AND FUTURE DEVELOPMENT

5.1 Limitations

There were some goal that was planned to be achieved by the end of the study, however there were several limitations that cannot be avoided during this study. First, the material; gelatine was supposed to be use is the industrial gelatine. However due to the origin of this industrial gelatine, the research assistance suggested that the gelatine need to be changed to different gelatine which was cooking gelatine. During the lab work, the 5 g and 10 g of inclusion were difficult to remove from the mould, and there was some residue of the gelatine left on the mould which make inclusion not spherical.

Next is time limitation. Due to the change of the gelatine, it took almost two weeks to find new gelatine and this have dragged so of the schedule. Besides that, all modalities ultrasounds and fibroscan were belongs to University Malaya Medical Centre and University Malaya Specialist Centre, therefore it were used to do the examination for patient too. The phantom scanning can only be done when there was no more patient on that day and Instron tensile machine can only be used when no other student used it. Due to time constraint, only one observer was managed to performed test using US Supersonics.

Instron tensile machine used was not microtester and commonly used for large sample. Since the machine was usually used for large sample, the distance between sample and the top-bottom plate need to be adjusted was hard to maintain as it need to manually set up, and this lead to error on the graph stress vs. strain plotted.

Lastly, lack of expertise on handling the instruments. During the measurement of fibroscan and instron, there was no sonographer and lab assistance that can be referred to

when problems encountered. Due to this, the radiologist has to refer to the manual when performing the scanning using fibroscan.

5.2 Future Development

For future development, more different shapes and sizes of inclusions could be constructed to investigate the effect parameter (shape) on elasticity by using SWE. Besides that, more SWI technique could be used to compare the data and determine the accuracy of each of the machine.

The phantom constructed was made from organic material and cannot be kept for long time even it was stored in the chiller. Therefore it is suggested to use different material that can be using to construct phantom.

CHAPTER 6: CONCLUSION

The elasticity of tissue using shear wave elastography (SWE) on three different modalities was performed using SWE (Philips and Supersonics) and Fibroscan®. Both elasticity and velocity values were obtained from US Philips meanwhile a homogeneous lesion was observed from colour map of US Supersonics. Homogeneous lesions varying in sizes were place on two different depth in order to determine factors affecting the elasticity. Based on measured data, size did not affect the elasticity however as the depth was deeper from the surface, elasticity was affected. Only graph from Supersonic imaging showed an increasing in elasticity as the mass of gelatine increased. At different depth and size, a 0.05 significant level paired t-test was performed and SWE Supersonics-Instron was significantly different between elasticity and mass of gelatin. It was observed that both mean elasticity of SWE Philips and SWE Supersonics were always higher than the elasticity measured by Instron.

REFERENCES

Chang, J. M., Moon, W. K., Cho, N., Yi, A., Koo, H. R., Han, W., … Kim, S. J. (2011). Clinical application of shear wave elastography (SWE) in the diagnosis of benign and malignant breast diseases. *Breast Cancer Research and Treatment*, *129*(1), 89–97. https://doi.org/10.1007/s10549-011-1627-7

D'angelo, E. (1975). Stress-strain relationships during uniform and nonauniform expansion of isolated lungs. *Respiration Physiology*, *23*(1), 87–107. https://doi.org/10.1016/0034-5687(75)90074-2

Dhyani, M., Anvari, A., & Samir, A. E. (2015). Ultrasound elastography: liver. *Abdominal Imaging*, *40*(4), 698–708. https://doi.org/10.1007/s00261-015-0373-4

Echosense. (2018). *Innovation in Liver Disease Management*. Retrieved from Fibroscan 502 Touch Echosense: http://www.echosens.us/fibroscan-502

Franchi-Abella, S., Elie, C., & Correas, J. M. (2013). Ultrasound elastography: Advantages, limitations and artefacts of the different techniques from a study on a phantom. *Diagnostic and Interventional Imaging*, *94*(5), 497–501. https://doi.org/10.1016/j.diii.2013.01.024

Friedrich-Rust, M., Schwarz, A., Ong, M., Dries, V., Schirmacher, P., Herrmann, E., … Sarrazin, C. (2009). Real-Time Tissue Elastography Versus FibroScan for Noninvasive Assessment of Liver Fibrosis in Chronic Liver Disease TT - Real-time-Elastografie versus FibroScan zur nicht invasiven Beurteilung des Leberfibrosestadium bei chronischer Lebererkrankung. *Ultraschall in Med*, *30*(5), 478–484. https://doi.org/10.1055/s-0028-1109488

Garra, B.S., Cespedes, E.L., Ophir, J., Spratt, S.R., Zuurbier, R.A., & Magnant, C.M. (1997). Elastography of breast lesions: *Initial clinical results, Radiology, 202(1),* 79-86.

Gennisson, J. L., Deffieux, T., Fink, M., & Tanter, M. (2013). Ultrasound elastography: Principles and techniques. *Diagnostic and Interventional Imaging*, *94*(5), 487–495. https://doi.org/10.1016/j.diii.2013.01.022

Jaffray, D. A. (2015). World Congress on Medical Physics and Biomedical Engineering, June 7-12, 2015, Toronto, Canada. *IFMBE Proceedings*, *51*, 252–253. https://doi.org/10.1007/978-3-319-19387-8

Jung, K. S., & Kim, S. U. (2012). Clinical applications of transient elastography. *Clinical and Molecular Hepatology*, *18*(2), 163. https://doi.org/10.3350/cmh.2012.18.2.163

Kemp, W., & Roberts, S. (2013). FibroScan and transient elastography. *Australian Family Physician*, *42*, 468–471. Retrieved from http://www.racgp.org.au/afp/2013/july/fibroscan/

Lee, E. J., Jung, H. K., Ko, K. H., Lee, J. T., & Yoon, J. H. (2013). Diagnostic performances of shear wave elastography: Which parameter to use in differential diagnosis of solid breast masses? *European Radiology*, *23*(7), 1803–1811. https://doi.org/10.1007/s00330-013-2782-5

Leschied, J. R., Dillman, J. R., Bilhartz, J., Heider, A., Smith, E. A., & Lopez, M. J. (2015). Shear wave elastography helps differentiate biliary atresia from other neonatal/infantile liver diseases. *Pediatric Radiology*, *45*(3), 366–375. https://doi.org/10.1007/s00247-014-3149-z

Maksuti, E., Widman, E., Larsson, D., Urban, M. W., Larsson, M., & Bjällmark, A. (2016). Arterial Stiffness Estimation by Shear Wave Elastography: Validation in Phantoms with Mechanical Testing. *Ultrasound in Medicine and Biology*, *42*(1), 308–321. https://doi.org/10.1016/j.ultrasmedbio.2015.08.012

Nightingale, R., Palmeri, K., Nightingale, M.R., & Trahey, G. (2001). *On the feasibility of remote palpation using acoustic radiation force*. *The Journal of the Acoustical Society of America* (Vol. 110). https://doi.org/10.1121/1.1378344

Ooi, C. C., Malliaras, P., Schneider, M. E., & Connell, D. A. (2014). "Soft, hard, or just right?" Applications and limitations of axial-strain sonoelastography and shear-wave elastography in the assessment of tendon injuries. *Skeletal Radiology*, *43*(1), 1–12. https://doi.org/10.1007/s00256-013-1695-3

Paparo, F., Corradi, F., Cevasco, L., Revelli, M., Marziano, A., Molini, L., … Rollandi, G. A. (2014). Real-Time Elastography in the Assessment of Liver Fibrosis: A Review of Qualitative and Semi-quantitative Methods for Elastogram Analysis. *Ultrasound in Medicine and Biology*, *40*(9), 1923–1933. https://doi.org/10.1016/j.ultrasmedbio.2014.03.021

Poynard, T., Pham, T., Perazzo, H., Munteanu, M., Luckina, E., Elaribi, D., … Castille, J. M. (2016). Real-time shear wave versus transient elastography for predicting fibrosis: Applicability, and impact of inflammation and steatosis. a non-invasive comparison. *PLoS ONE*, *11*(10), 1–16. https://doi.org/10.1371/journal.pone.0163276

Samuel, D. (2016). Retrieved from Dr Douglas Samuel Gastroenterologist and Consultant Physician: http://www.dougsamuel.com.au/fibroscan/

Sarvazyan, A. P. (1995a). *Biophysical bases of elastic imaging* (Vol. 21). New York: In:Acoustical Imagine

Sporea, I., Sirli, R., Deleanu, A., Iulia, R., Tudora, A., Dan, I., & Popescu, A. (2011). What did we learn from the first 3,459 cases of liver stiffness measurement by transient elastography (fibroscan)? *Scopus*, *32*(1), 40-45. doi:10.1055/s-0029-1245525

Wilder, J., & Patel, K. (2014). The Clinical Utility of Fibroscan® as a Noninvasive Diagnostic Test for Liver Disease. *Medical Devices: Evidence and Research*, 107-114. doi:10.2147/MDER.S46943

Wells, P., & Liang, H. (2011). Medical ultrasound: imaging of soft tissue strain and elasticity. *Journal of The Royal Society Interface*, (June), 1–29. https://doi.org/10.1098/rsif.2011.0054

Yeh, W.-C., Li, P.-C., Jeng, Y.-M., Hsu, H.-C., Kuo, P.-L., Li, M.-L., … Lee, P. H. (2002). Elastic modulus measurements of human liver and correlation with pathology. *Ultrasound in Medicine and Biology*, *28*(4), 467–474. https://doi.org/10.1016/S0301-5629(02)00489-1s

Yeong, C. H., Abdullah, B. J. J., Ng, K. H., & Ting, C. E. (2015). Accuracy of Tissue Elasticity Measurement Using Shear Wave Ultrasound Elastography: Comparison With Gold Standard. *European Society of Radiology*, *Scientific*, 1–20. https://doi.org/10.1594/ecr2015/C-0542